Supporting Information for

Uncertainty-weighted fuzzy clustering disentangles climate-stress VOC fingerprints and associated stress-dependent temperature sensitivity in urban trees

Biplob Dey[1,3], Clémence Depp[1,2], Yichen Gu[1], Anna Novelli[1], Hendrik Fuchs[1,4], Thorsten Hohaus[1], Eva Y. Pfannerstill[1,2,*]

[1]Institute of Climate and Energy Systems: Troposphere (ICE-3), Forschungszentrum Jülich, Jülich, Germany
[2]Institute of Geophysics and Meteorology, University of Cologne, Cologne, Germany
[3]Bioclimatology, Faculty of Forest Sciences and Forest Ecology, University of Göttingen, Göttingen, Germany
[4]Department of Physics, University of Cologne, Cologne, Germany

Correspondence: Eva Y. Pfannerstill (e.pfannerstill@fz-juelich.de)

Table of contents

01. VOC-carbon dynamics 2
02. Gas chromatography (GC) based attribution 3
03. UWFCM cluster resolution and cluster selection 3
04. Inlet positioning and implications for PTR-ToF-MS measurements 10
05. Temperature-dependent emission factor 11
06. SAPHIR-PLUS chamber 15
07. Cluster-resolved stress fingerprints 16
08. Detection limit of the FUSION PTR-TOF-MS compounds 20
09. References 22

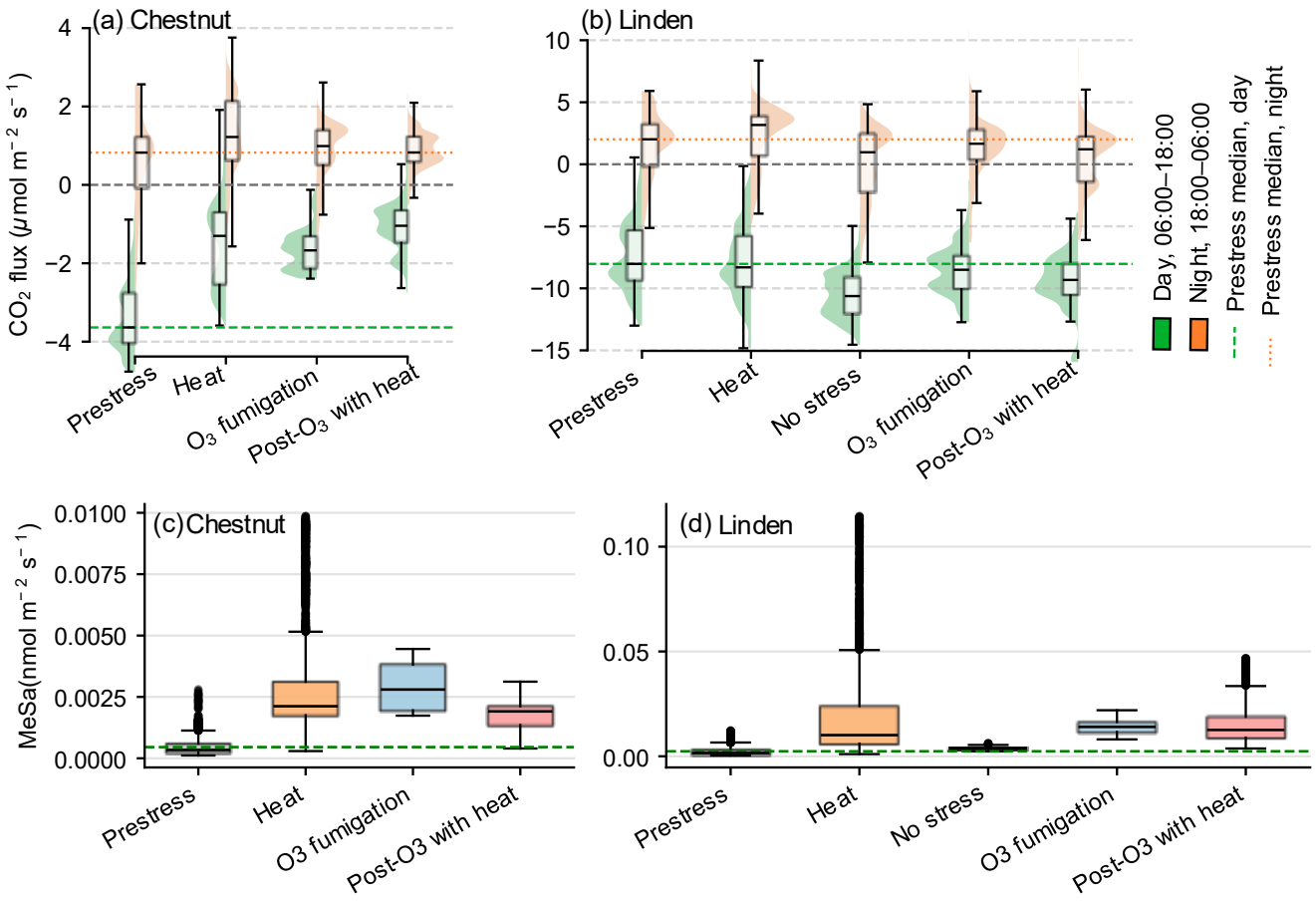


Figure S1 Measured CO_2 assimilation and methyl salicylate (MeSa) emissions rates in chestnut and linden under different stress including pre-stress (no stress). Subplot (a–b) show daytime and nighttime CO_2 assimilation rates for chestnut and linden, respectively. Half-violin plots represent the data distribution, and boxplots indicate the median and interquartile range. Horizontal lines indicate prestress daytime and nighttime median assimilation rate. Subplots (c–d) show MeSa emissions, and the boxplots indicate the median, interquartile range, and outliers.

Table S1 Mean (μmol m^{-2} s^{-1}) daytime CO_2 uptake, nighttime CO_2 exchange, and net CO_2 balance of chestnut and linden. Negative values indicate net CO_2 uptake (carbon sink), whereas positive values indicate net CO_2 release (carbon source).

Species	Stress	Daytime	Nighttime	Net CO_2 balance
Chestnut	Prestress	-3.378	0.547	-2.831
Chestnut	Heat	-1.541	1.21	-0.331
Chestnut	O3 fumigation	-1.645	0.843	-0.801
Chestnut	Post-O3 with heat	-1.095	0.86	-0.235
Linden	Prestress	-7.347	1.544	-5.803
Linden	Heat	-7.847	2.263	-5.584
Linden	No stress	-10.539	-0.043	-10.582
Linden	O3 fumigation	-8.626	1.292	-7.334
Linden	Post-O3 with heat	-9.457	0.485	-8.972

02. Gas chromatography (GC) based attribution

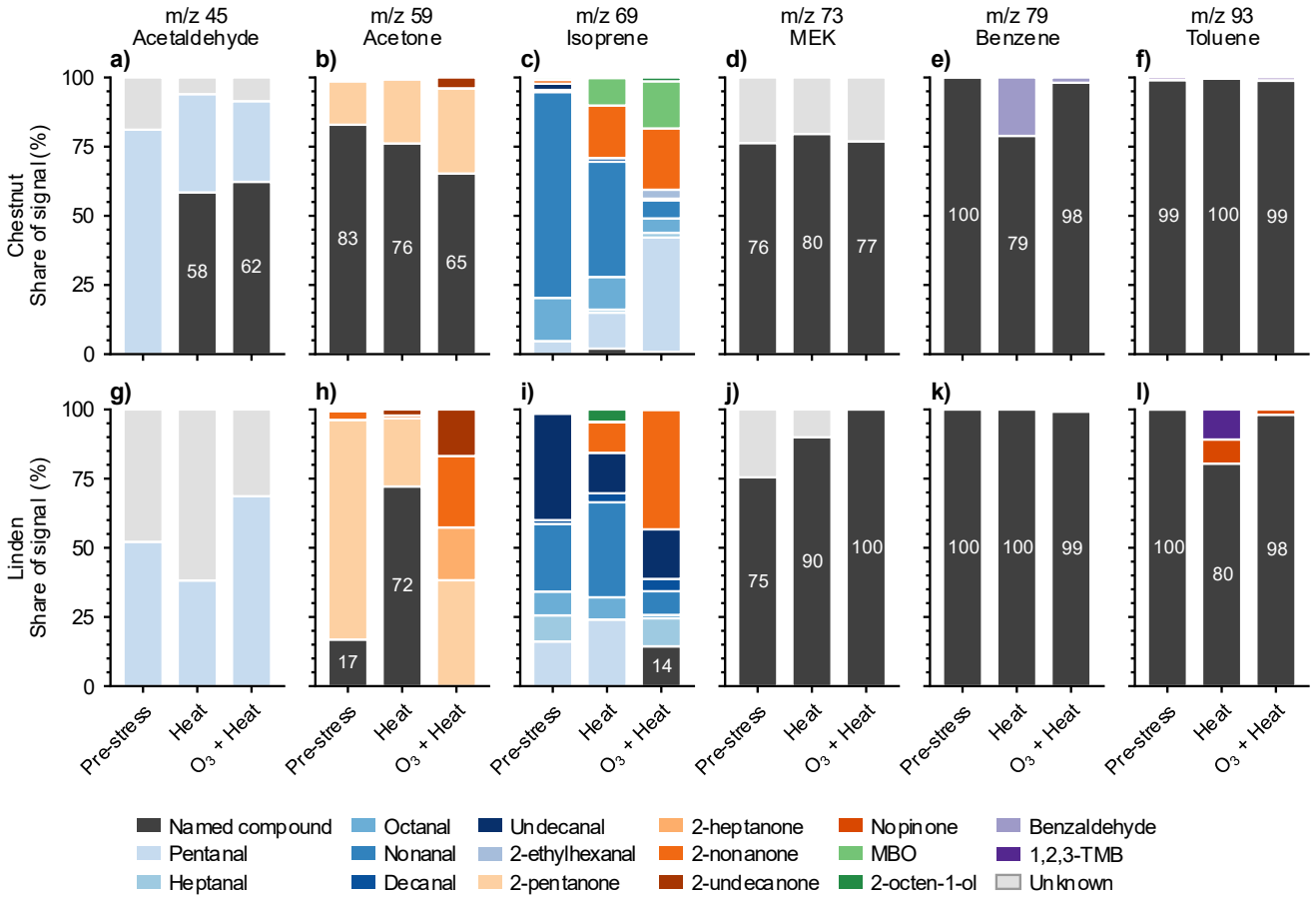


Figure S2 GC-resolved composition of PTR-ToF-MS ion signals. Stacked bars show the share of each ion's signal attributed to the compounds detected by online GC-MS, for chestnut (a-f) and linden (g-i) in each stress including pre-stress. Stacked bars show the contributions of individual compounds, with dark grey representing the assigned compound and light grey indicating unidentified contributions.

03. UWFCM cluster resolution and cluster selection

To identify the optimal cluster solution, candidate solutions were systematically evaluated across 2 to 10 cluster solutions and fuzziness coefficients ranging from 1.2 to 2.0, using multiple complementary statistical criteria and biological interpretability. As an initial evaluation, clustering performance was evaluated using the fuzzy partition coefficient (FPC) and partition entropy (PE) (Fig. S3). FPC quantifies the degree of cluster separation, with values approaching 1 indicating highly distinct clusters and reduced overlap. In both chestnut and linden emissions, FPC decreased progressively as the number of clusters increased, showing the expected decrease in compactness when more partitioning is applied (Fig.S3 a,d). Although the highest FPC values and lowest PE values were found for low-dimensional cluster solutions (c = 2-3), these indices primarily quantify partition certainty and do not necessarily capture the underlying biological structure. Similar limitations of partition-based validity measures have been noted previously[1], in which statistically favorable solutions may fail to reflect the true cluster because they emphasize membership concentration rather than cluster geometry and interpretability[2]. Partition entropy was also evaluated and increased periodically with increasing the cluster number and fuzziness parameter (Fig. S3 b,e). Low-cluster solutions showed the lowest entropy values, indicating highly certain memberships. Nevertheless, low entropy alone does not imply biologically meaningful clustering because a trivial separation of stressed and non-stressed states can simultaneously produce low uncertainty. Therefore, FPC and PE were interpreted primarily as indicators of clustering stability rather than as sole criteria for cluster selection.

Fuzzy c-means clustering is based on distances in multidimensional feature space, the resulting cluster geometry can be sensitive to data transformation and scaling[3,4]. VOC emission from plants changed substantially across time and stress, with variance and signal-to-noise ratio. To evaluate whether the identified clusters and fingerprint spectra reflected intrinsic biological structure rather than preprocessing-induced artifacts, the assessment was conducted across 3 data transformation techniques as discussed earlier in the methods and evaluated using the fuzzy adjusted rand index (Fig. S3c,f). The strongest agreement was found between c = 4 and c = 6 (Fig. S3c,f). These solutions represent stable and reproducible VOC emission fingerprints rather than transformation-dependent artifacts. Fuzzy silhouette, Davies–Bouldin index, Bootstrap ARI, and membership entropy showed that the cluster stability and separation improved between clusters 5 and 6 (Fig. S4). Further details on these clustering validation indices are provided in Wu et al.[5].

Biological interpretability was evaluated based on the temporal profile and spectral composition of clusters across candidate solutions (Fig. S5-S7). In both chestnut (Fig.S5) and linden (Fig.S7), the two-cluster solution generally differentiated between constitutive and stress-related emissions but did not distinguish individual stress states, as clusters remained active across multiple stress periods. Increasing the number of cluster solution to 3 and 4 gradually showed additional emission patterns; however, several clusters still showed overlapping temporal responses and mixed spectral features (confirmed by cosine similarity index), which limit their interpretation as distinct stress indicators.

The five-cluster solution was the first to show that all major stress phases could be differentiated by distinct temporal patterns and related mass spectral profiles. In chestnut, cluster-1 dominated the pre-stress period, whereas clusters 2–4 captured emissions associated with heat exposure and transitional stress responses (Fig.S5). Cluster-5 coincided with the heat+O_3 phase and showed a distinct spectral signature (Fig.S6) not resolved in lower-dimensional solutions, indicating the appearance of an additional stress-related emission factor. A similar pattern was observed for linden (Fig. S7), where the five-cluster solution separated constitutive heat-responsive emissions, which aligned with the treatment boundaries. Cluster 5 has a coherent temporal pattern and a unique spectral fingerprint, rather than a simple fragment of an existing cluster (Fig.S6).

Based on the combined clustering evaluation as discussed, the five-cluster UWFCM solution was selected for subsequent analysis. While solutions with more than five clusters were also evaluated, the additional clusters largely represented fragmentation of the existing factor solution rather than distinct stress-related factors.

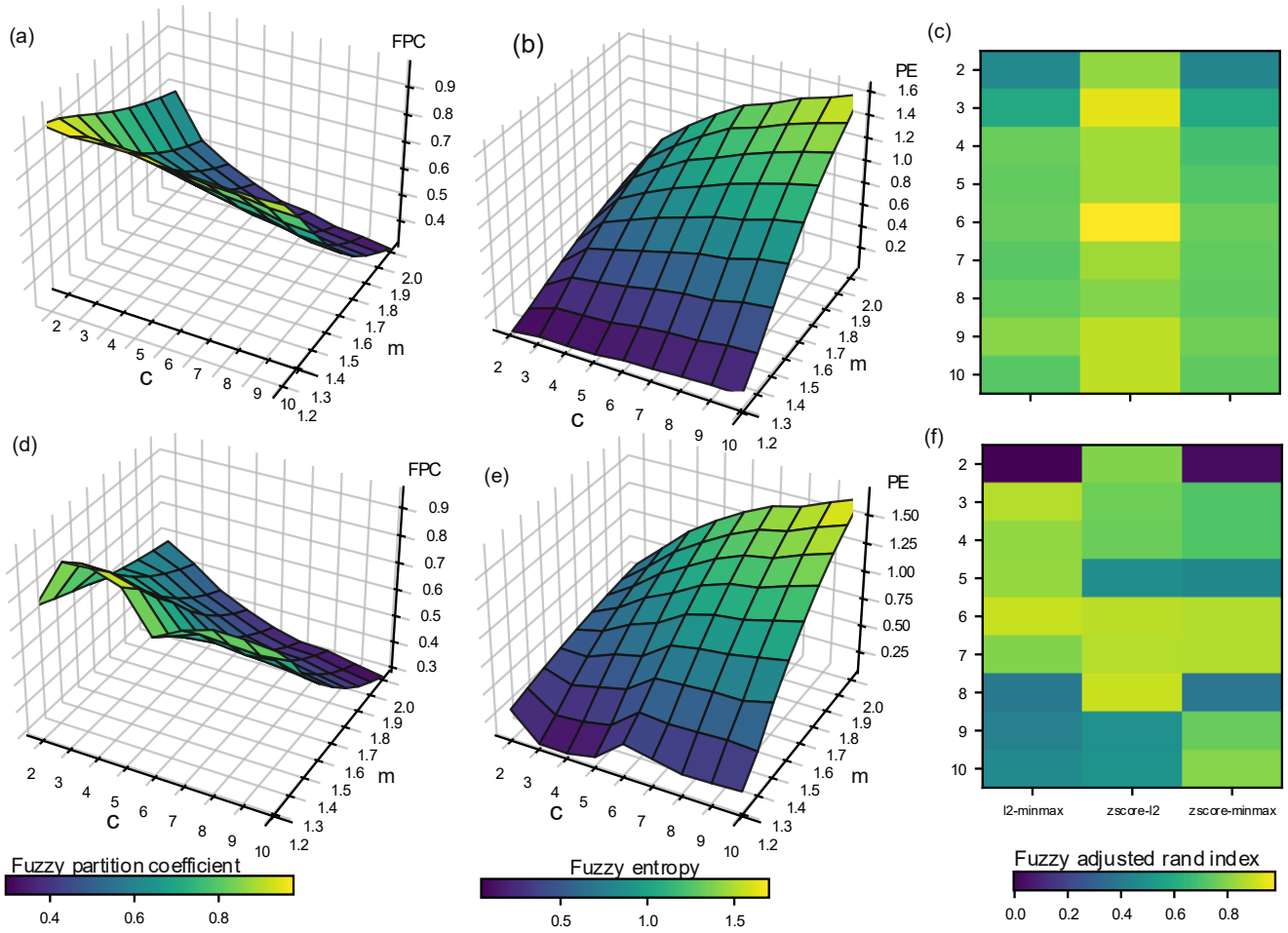


Figure S3 Fuzzy clustering evaluation metrics across cluster number (c) and fuzziness parameter (m) for chestnut (a-c) and linden (d-f). Subplots (a,d) show the fuzzy partition coefficient (FPC), where higher values indicate stronger cluster separation, while subplots (b,e) show partition entropy (PE), where lower values indicate reduced membership uncertainty. Subplots (c,f) show heatmaps of clustering agreement between preprocessing transformations, measured using the fuzzy adjusted rand index (ARI) across different cluster numbers. The evaluated preprocessing combinations include L2 (Euclidean) normalization + min–max scaling, z-score + L2 normalization, and z-score + min–max scaling. Higher ARI values indicate greater clustering consistency between preprocessing methods.

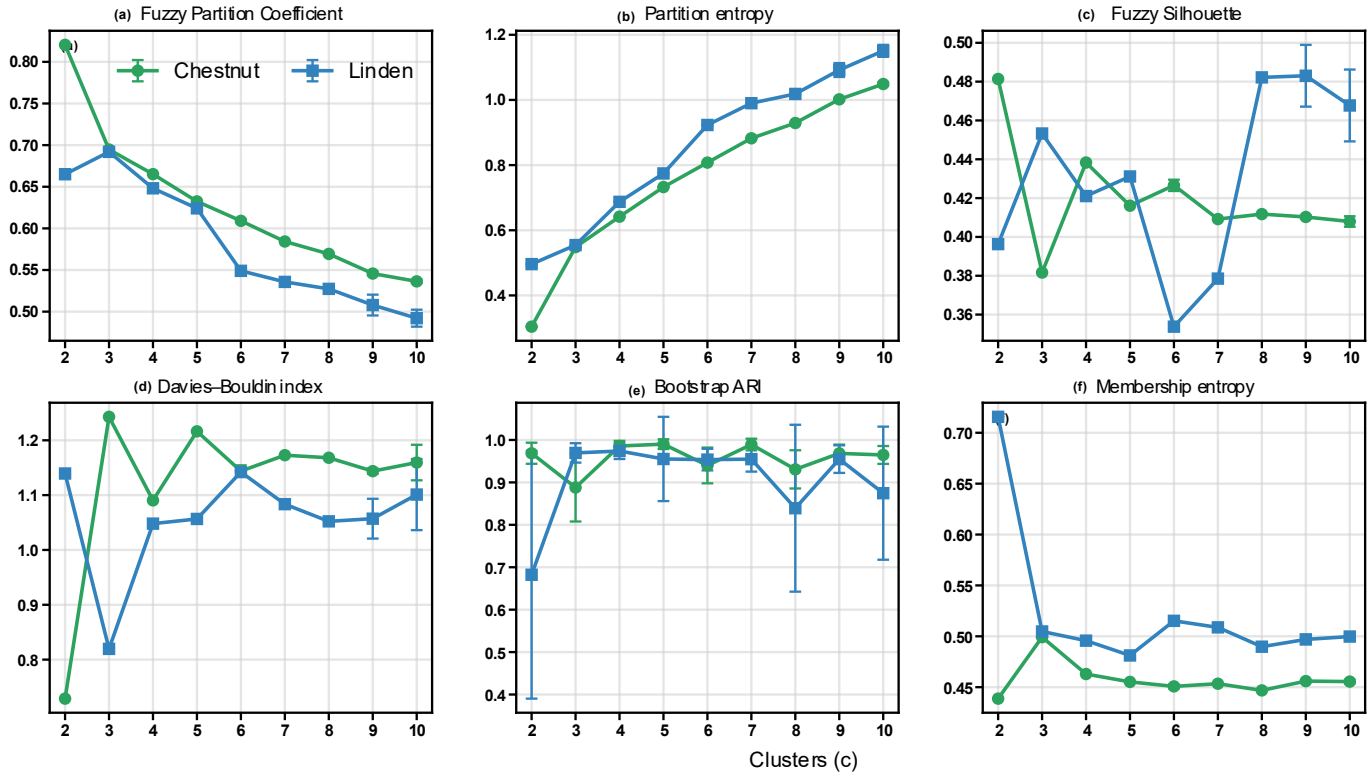


Figure S4 Fuzzy clustering evaluation metrics comparison across cluster numbers (c=2–10) for chestnut and linden. Subplot shows (a) fuzzy partition coefficient (FPC), (b) partition entropy (PE), (c) fuzzy silhouette, (d) davies–bouldin index (DB), (e) bootstrap adjusted rand index (Bootstrap ARI), and (f) membership entropy. Error bars represent standard deviation across bootstrapping. Higher index values show better clustering performance for FPC, fuzzy silhouette, and bootstrap ARI, whereas lower values indicate better performance for PE, DB, and Membership entropy.

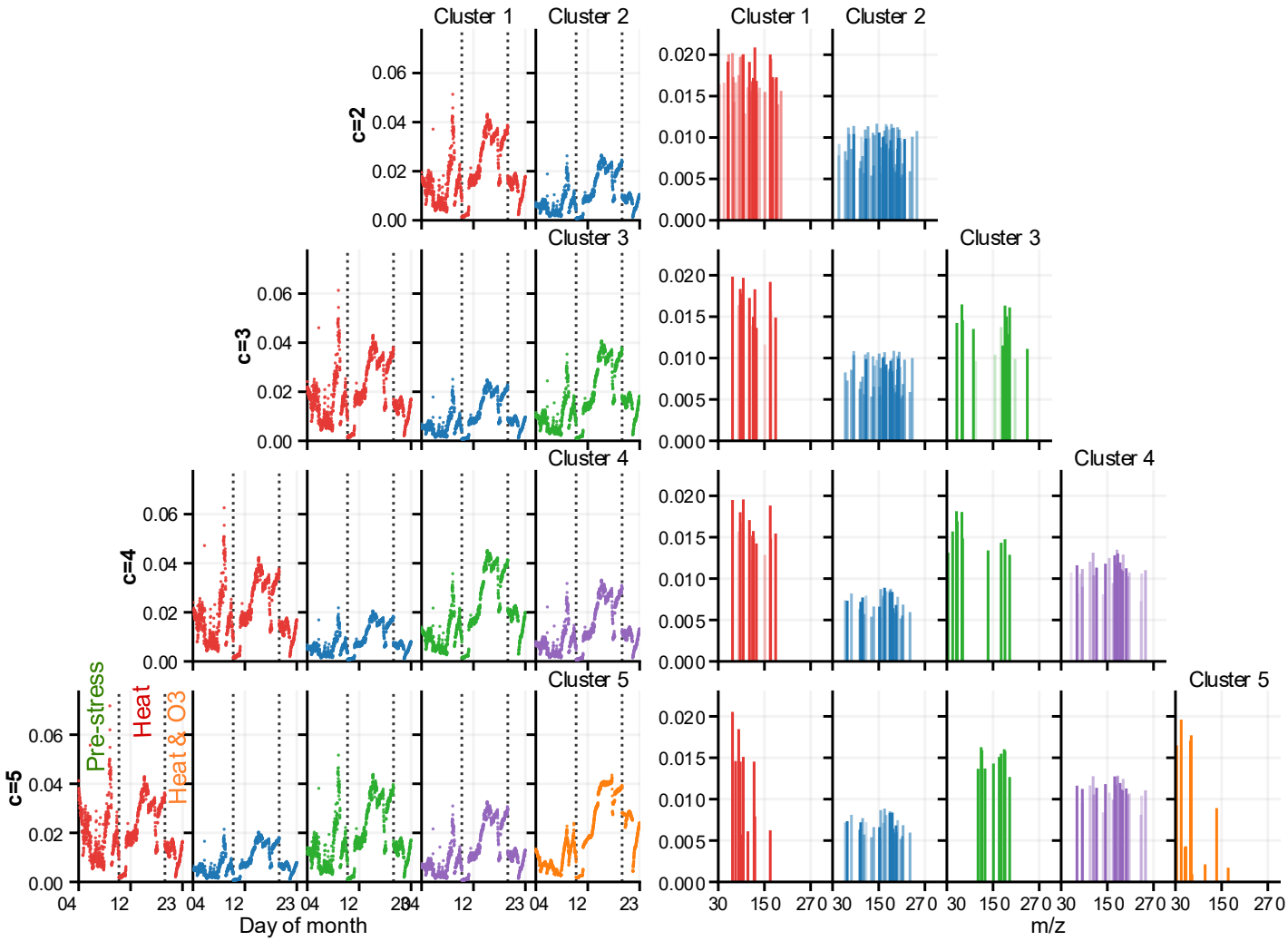


Figure S5 Different cluster-specific temporal and mass spectra from uncertainty-weighted fuzzy c-means clustering of chestnut. Temporal profiles (left) and corresponding mass spectra (right) are shown for fuzzy c-means solutions ranging from c = 2 to c = 5. Each row represents a different cluster solution, and each colored panel corresponds to an individual cluster within that solution. Temporal panels show normalized cluster-associated signal intensity across the stress period, with vertically dotted lines indicating transitions between stress. Spectral panels show the corresponding normalized m/z distributions.

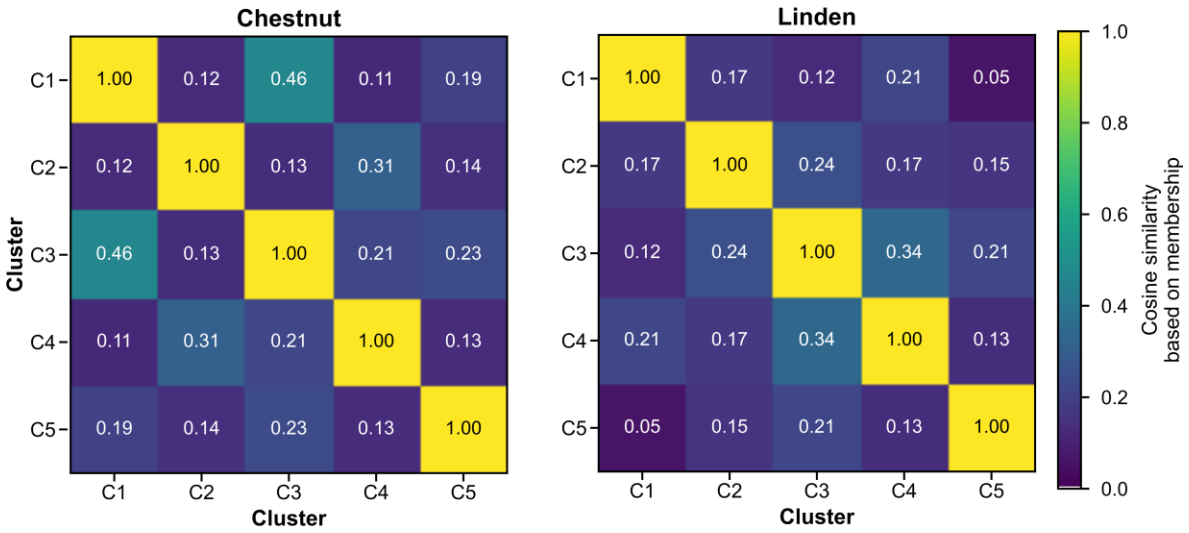


Figure S6 Cosine similarity index of fuzzy cluster membership profiles for chestnut and linden based on the 5-cluster solution. Similarity was calculated using cosine similarity between cluster-specific membership vectors.

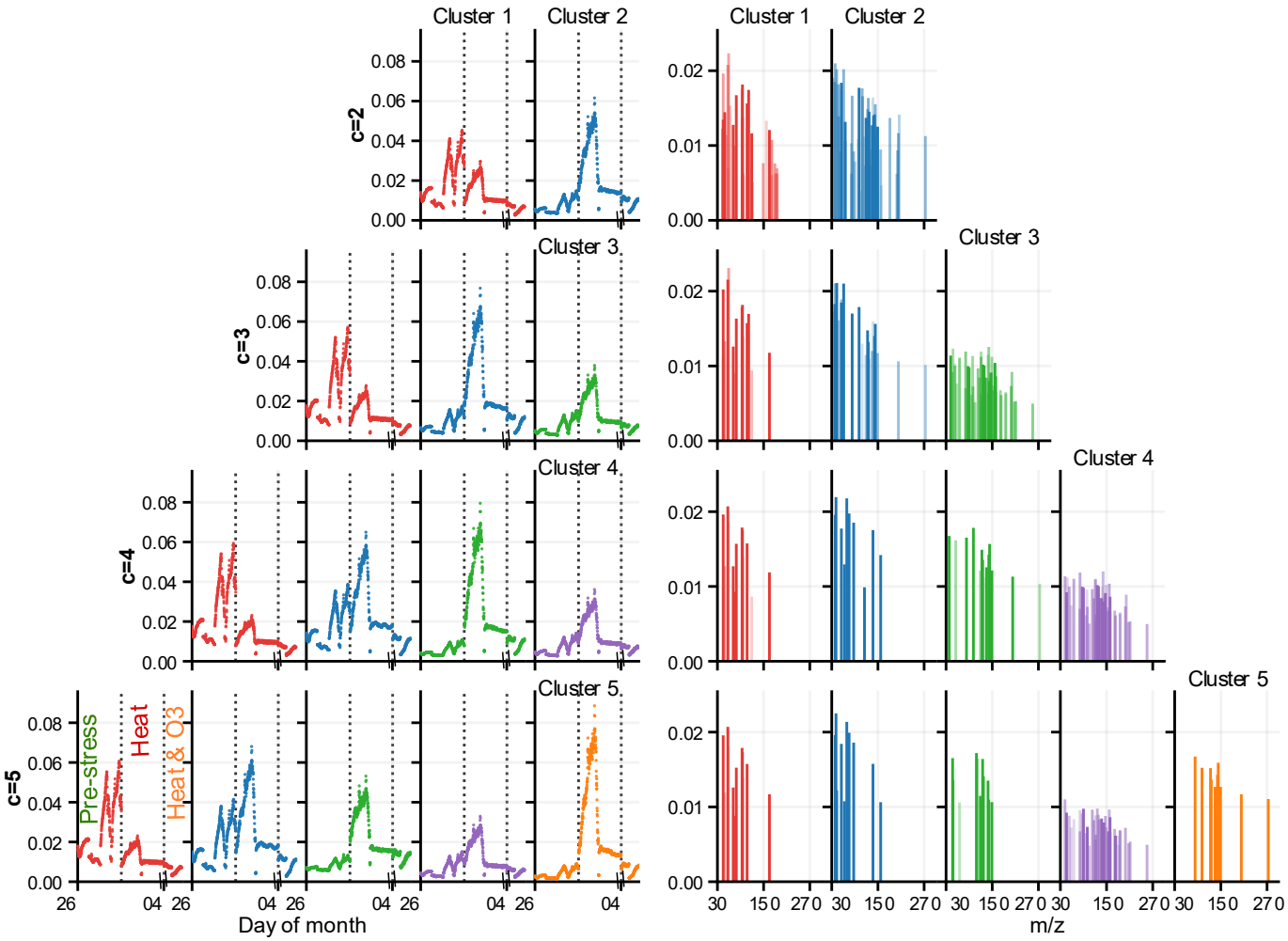


Figure S7 Different cluster-specific temporal and mass spectra from uncertainty-weighted fuzzy c-means clustering of linden. Temporal profiles (left) and corresponding mass spectra (right) are shown for fuzzy c-means solutions ranging from c = 2 to c = 5. Each row represents a different cluster solution, and each colored panel corresponds to an individual cluster within that solution. Temporal panels show normalized cluster-associated signal intensity across the stress period, with vertically dotted lines indicating transitions between stress. Spectral panels show the corresponding normalized m/z distributions.

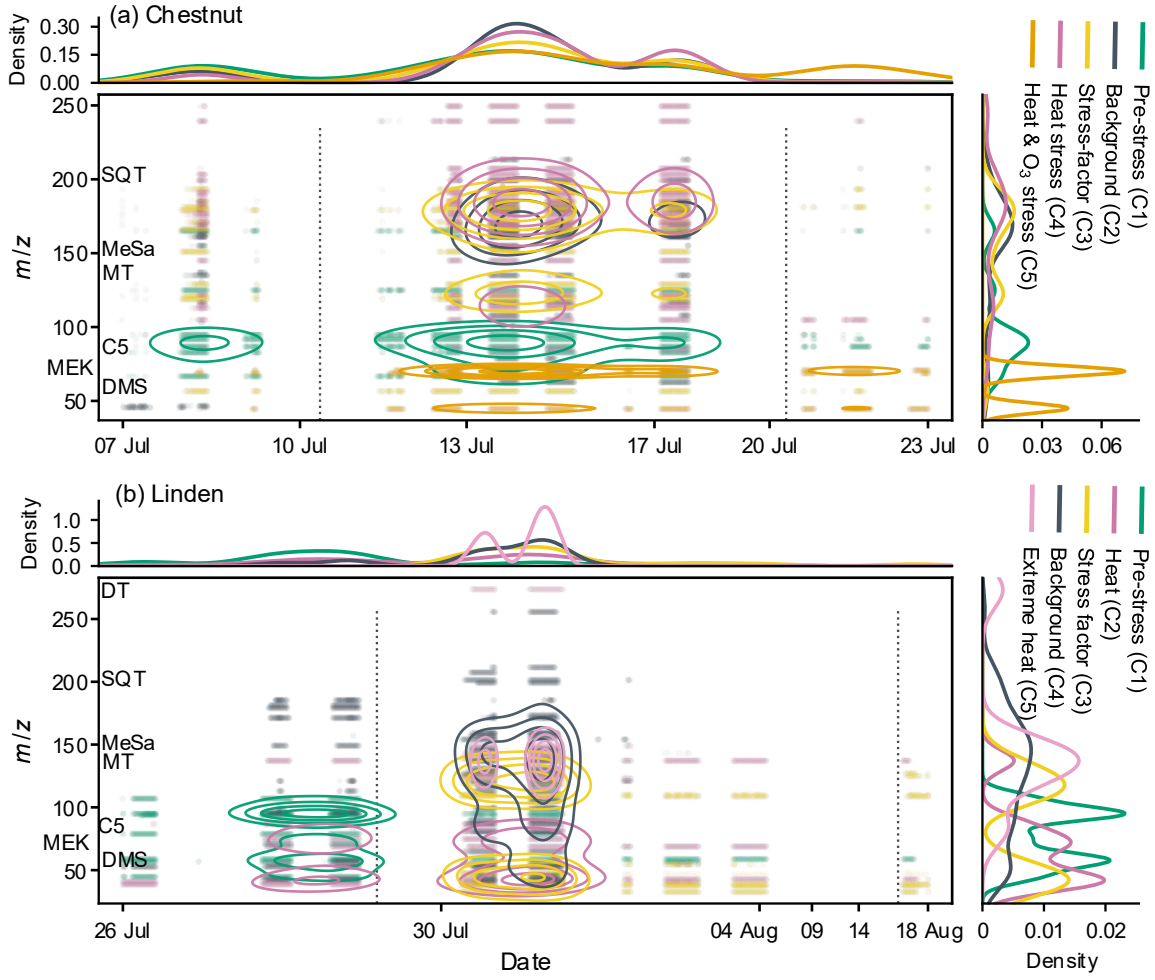


Figure S8 Temporal–spectra distributions of VOC emissions of 5 factor solution by UWFCM for chestnut (a) and linden (b). Panels show the distribution of different compounds across time and points represent individual weighted observations, while colored contour lines indicate two-dimensional Gaussian kernel density estimates for each cluster in time-m/z space. Marginal density plots above and to the right summarize the temporal and m/z distributions, respectively. Vertical dotted lines show the stress transition from prestress, heat and combined heat ozone stress.

04. Inlet positioning and implications for PTR-ToF-MS measurements

During the chestnut experiment (4-25 July 2025), the FUSION PTR-ToF-MS inlet was pulled out of its intended position. This caused the instrument to inadvertently sample air from the interspace behind the inlet connection and between two air-filled layers of polytetrafluoroethylene foil of the PLUS chamber rather than directly from the chamber air. Consequently, VOCs may have been retained in the interspace that acts as a reservoir and subsequently released with a delay, leading to dampened signals. To reconstruct the direct, undampened plant emission signals, several signal reconstruction approaches were assessed, (i.e considering an interspace dead volume reservoir, inlet-loss factor) and compared with independently measured OH reactivity by laser photolysis–laser-induced fluorescence (LP-LIF). However, none of these approaches consistently reproduced the measured OH reactivity (when calculating reactivity from PTR-ToF-MS observations) without introducing new biases. We therefore used the uncorrected chestnut measurements to avoid introducing model-dependent assumptions into the analysis. The FUSION inlet was repositioned on 30 July 2025, before the linden heat stress measurements, which were therefore unaffected by this inlet-positioning issue. Although this choice preserves the original observations, potential biases with reduced absolute emission rates and a dampened diel variability are expected for the

chestnut data. None of this affects the reported relative changes or the UWFMC fingerprinting model. Therefore, no model-based signal reconstruction was applied, and the original PTR-ToF-MS measurements were used for analysis.

05. Temperature-dependent emission factor

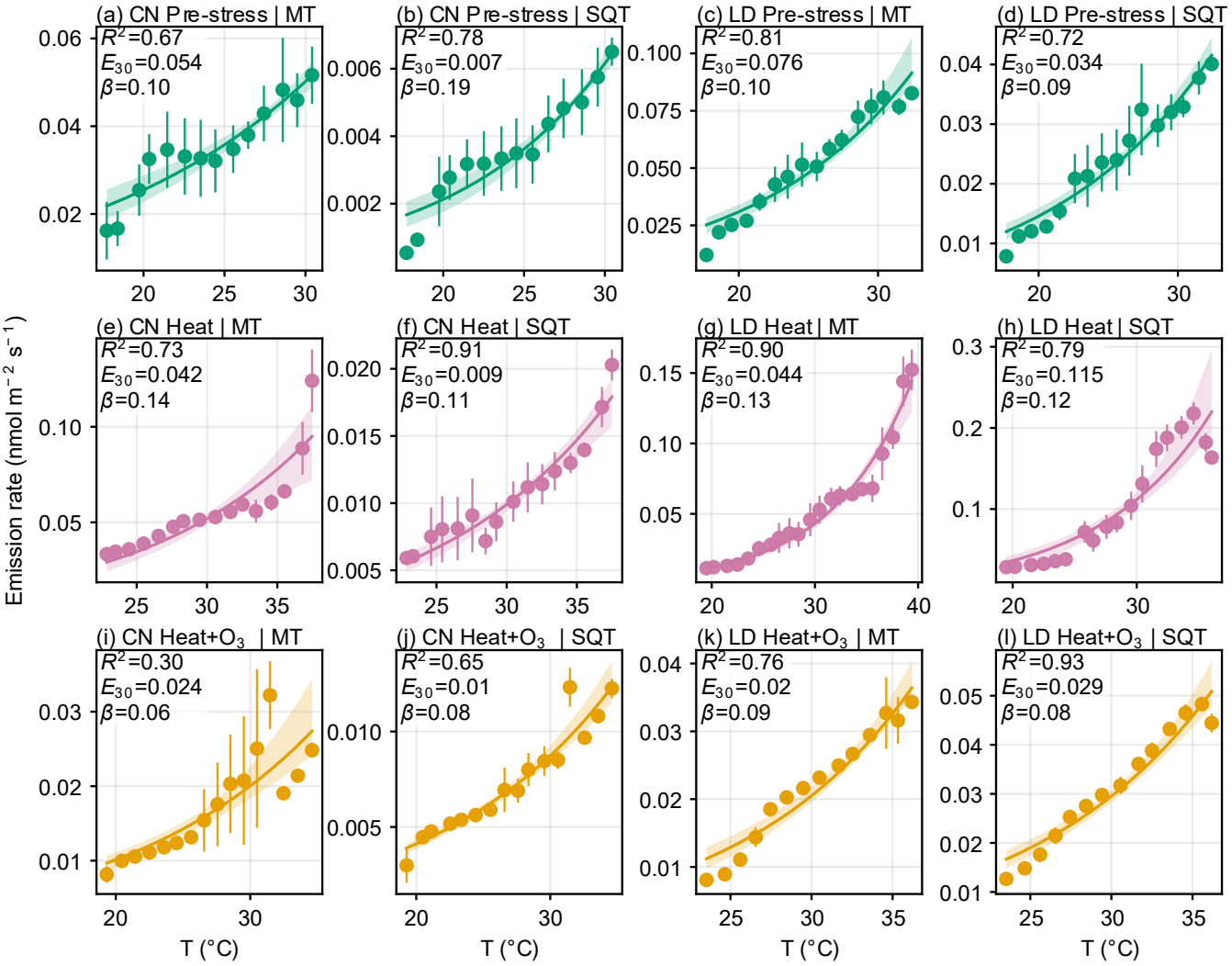


Figure S9 Temperature dependence of monoterpenes (MT; m/z 137.13) and sesquiterpenes (SQT; m/z 205.19) emissions under stress. Emission rates are shown as a function of temperature for chestnut and linden under pres-stress, heat stress, and combined heat + ozone stress. Points represent binned means (± sd), and lines show exponential fits $E = E_{30}\exp[\beta(T - 30)]$ and the shaded area represents 5–95% bootstrap confidence intervals.

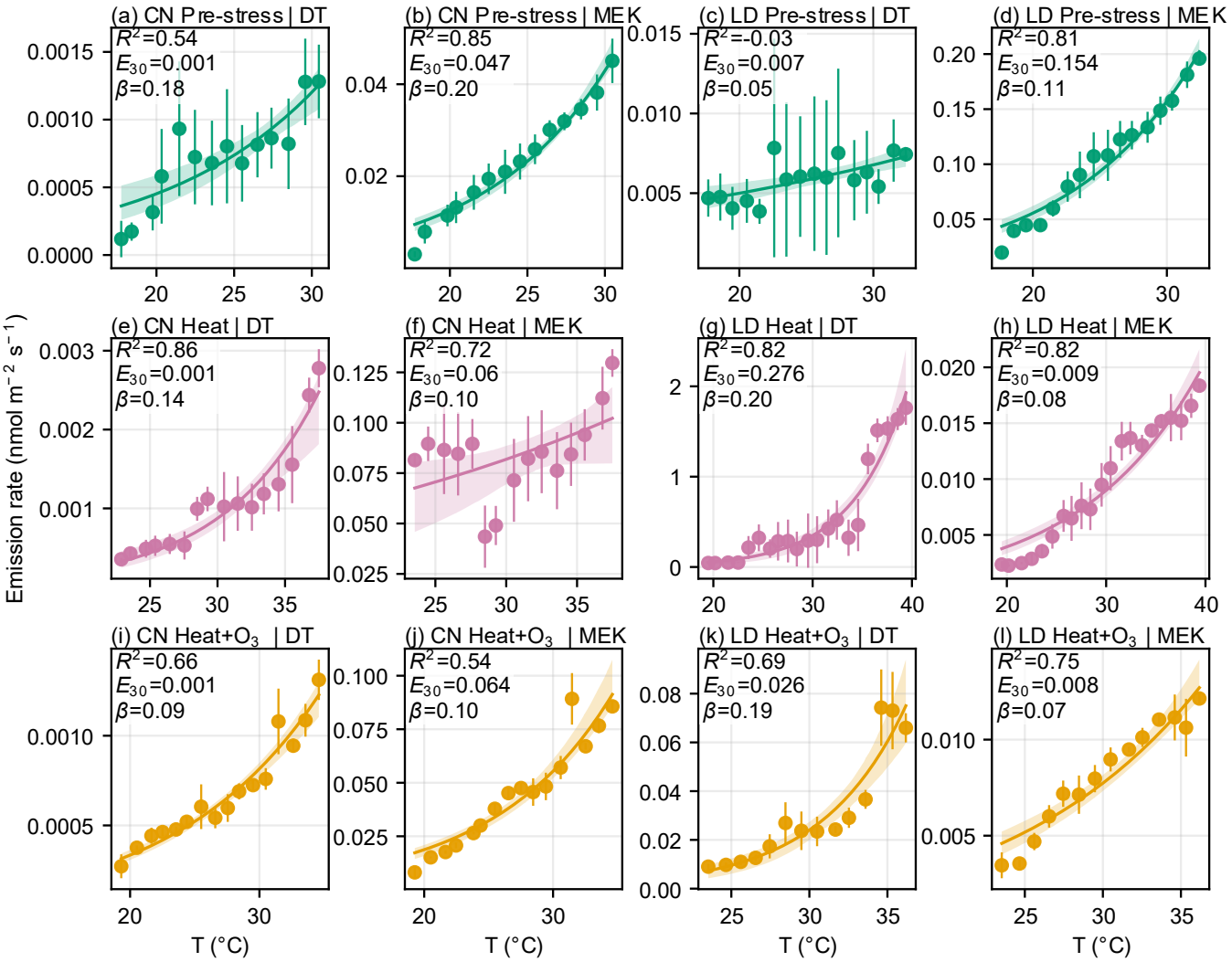


Figure S10 Temperature dependence of diterpenes (DT; m/z 273.25) and methyl ethyl ketone (MEK; m/z 73.06) emissions under stress. Emission rates are shown as a function of temperature for chestnut and linden under pre-stress, heat stress, and combined heat + ozone stress. Points represent binned means (± sd), and lines show exponential fits $E = E_{30}\exp[\beta(T - 30)]$ and the shaded area represents 5–95% bootstrap confidence intervals.

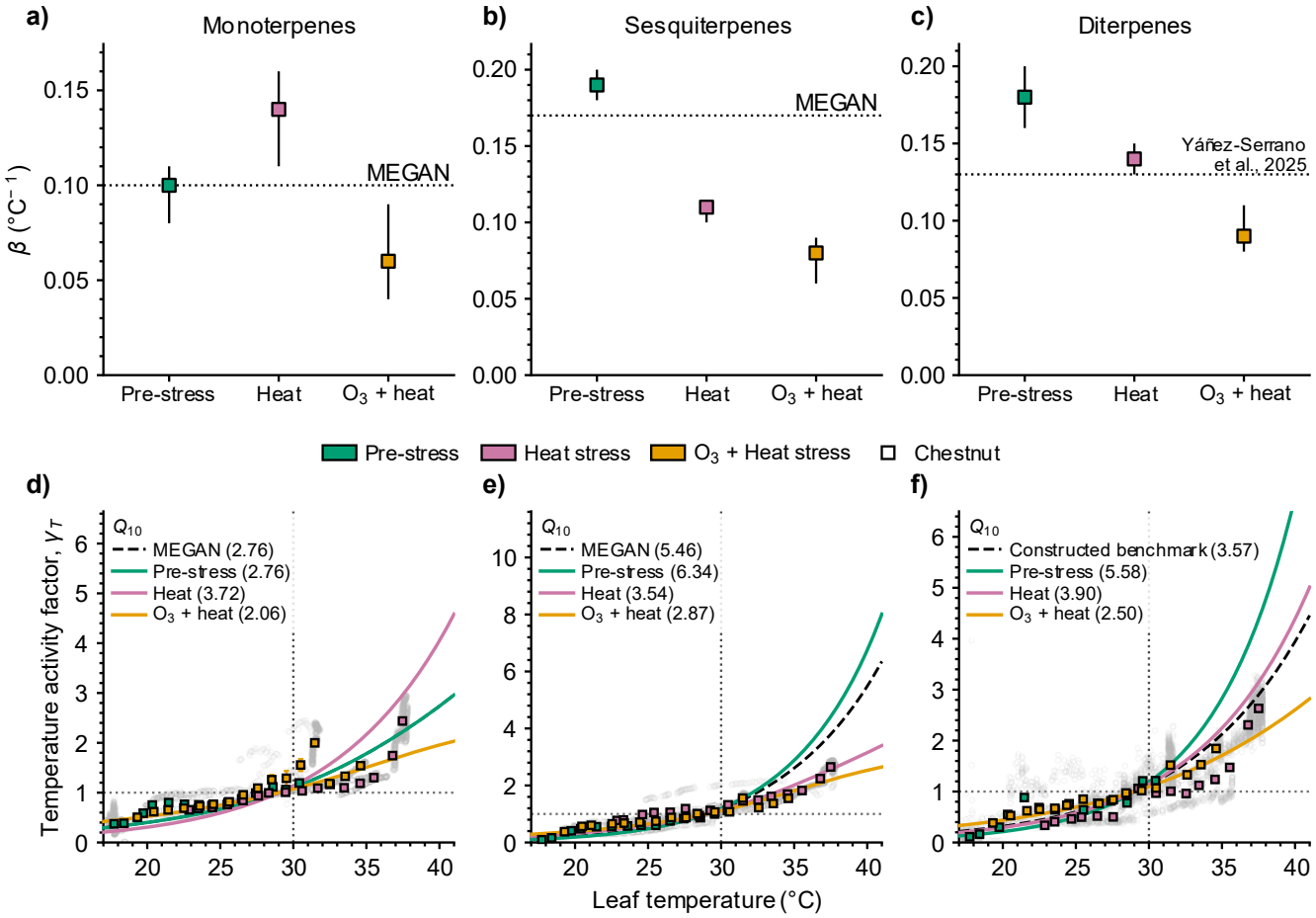


Figure S11 Stress-dependent temperature responses of terpenoid emissions for chestnut. (a–c) Temperature sensitivity coefficients (β) for monoterpenes, sesquiterpenes and diterpenes, respectively, under pre-stress, heat stress and combined ozone-heat stress conditions. Points represent recommended β values from β exponential fits, and error bars represent the supported β range within 5% of the minimum RMSE. (d–f) Corresponding temperature activity factors (γ_t) as a function of leaf temperature. Grey circles represent individual normalized emission measurements from chestnut species, and coloured squares indicate 1 °C temperature-bin means ± standard error. Solid curves show stress-specific temperature-response functions derived from MEGAN-based parameterizations, while dashed black curves indicate the reference MEGAN functions or, for diterpenes, a constructed benchmark. Q10 (dimensionless) is the multiplicative change in emission rate per 10 K. Vertical and horizontal dotted lines mark the reference temperature (30 °C) and normalized activity factor (γ_t = 1), respectively.

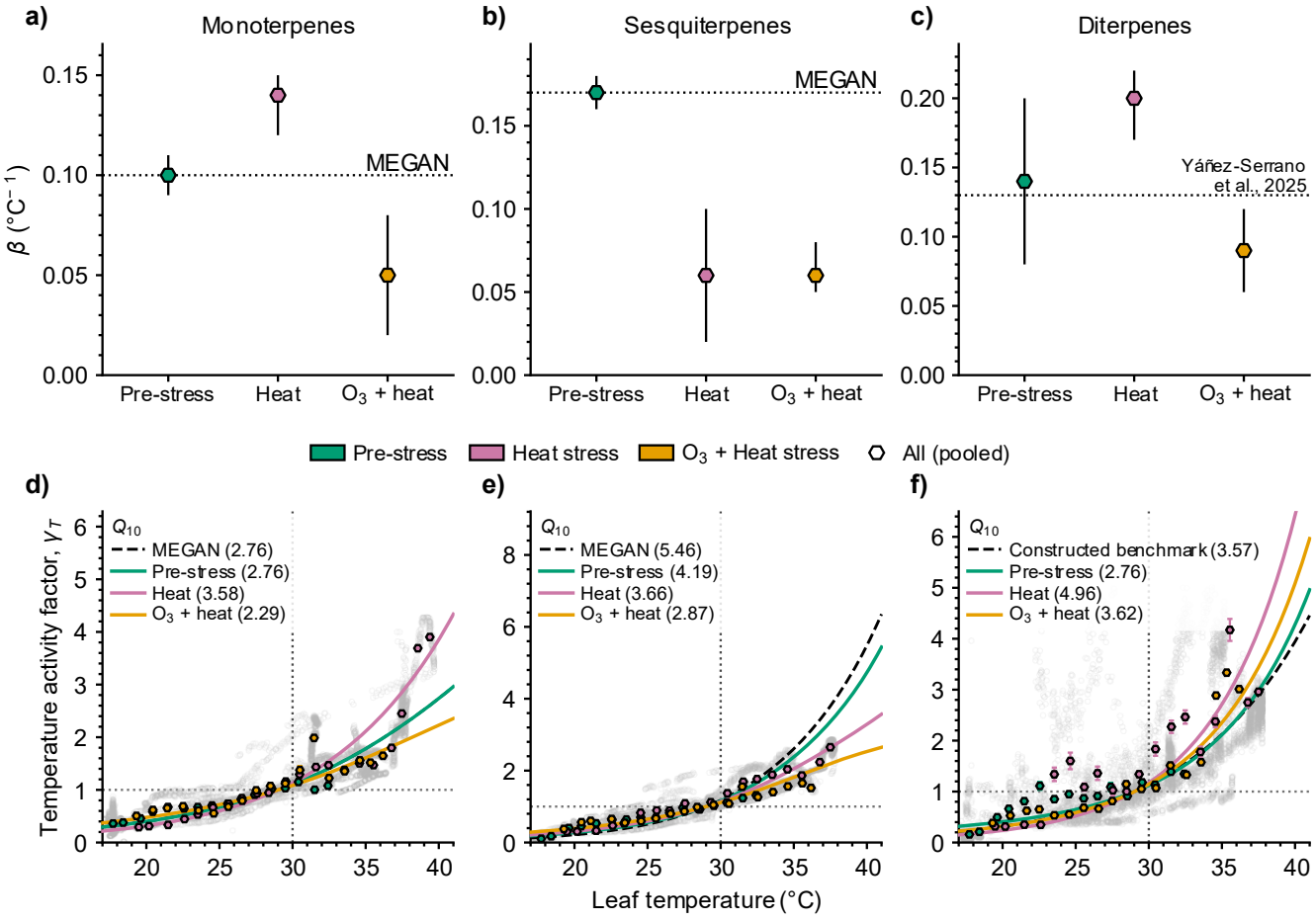


Figure S12 Stress-dependent temperature responses of terpenoid emissions. (a–c) Temperature sensitivity coefficients (β) for monoterpenes, sesquiterpenes and diterpenes, respectively, under pre-stress, heat stress and combined ozone-heat stress conditions from pooled datasets (from both chestnut and linden). Points represent recommended β values from β exponential fits, and error bars represent the supported β range within 5% of the minimum RMSE. (d–f) Corresponding temperature activity factors (γ_t) as a function of leaf temperature. Grey circles represent individual normalized emission measurements from both species, and coloured squares indicate 1 °C temperature-bin means ± standard error. Solid curves show stress-specific temperature-response functions derived from MEGAN-based parameterizations, while dashed black curves indicate the reference MEGAN functions or, for diterpenes, a constructed benchmark. Q10 (dimensionless) is the multiplicative change in emission rate per 10 K. Vertical and horizontal dotted lines mark the reference temperature (30 °C) and normalized activity factor ($\gamma_t = 1$), respectively.

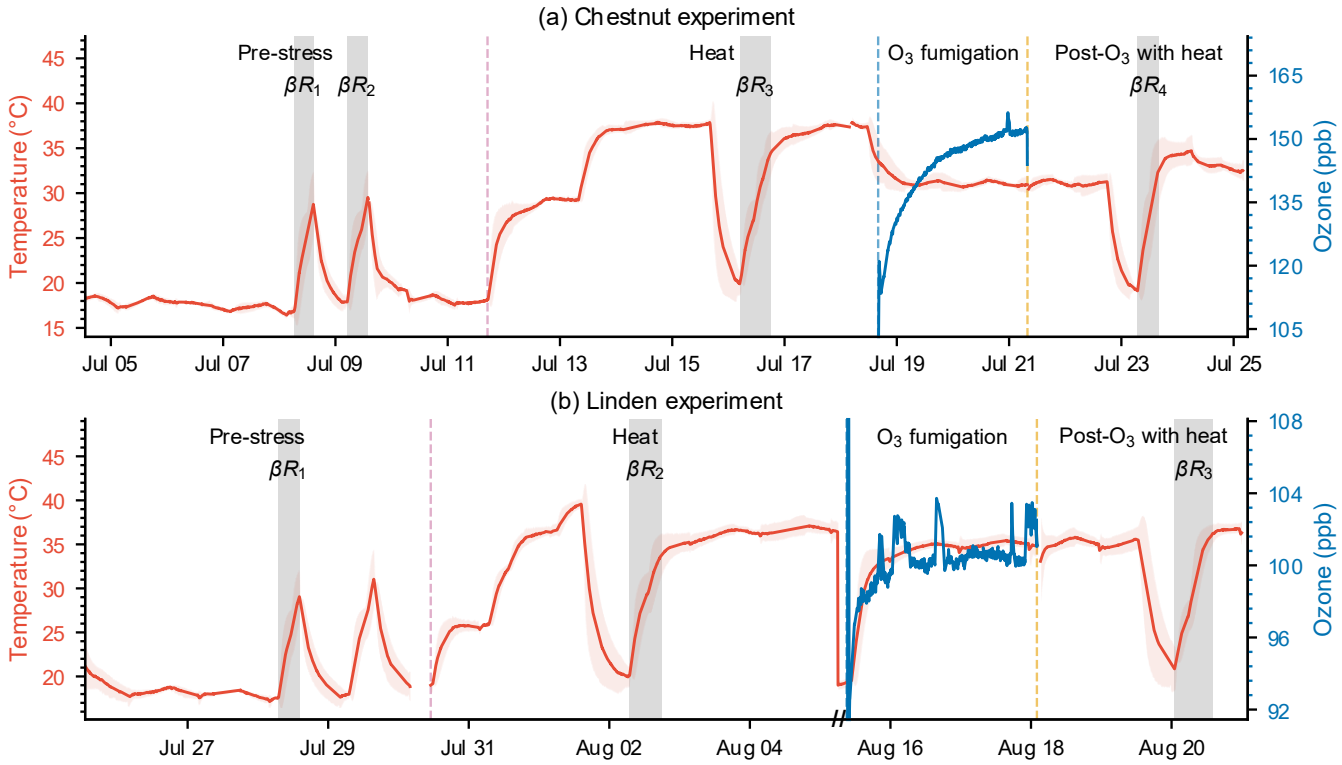


Figure S13 Experimental timelines of the (a) chestnut and (b) linden plant chamber stress experiment. Red lines show air temperature in the plant chamber, and blue lines represent the injected ozone concentrations during the fumigation periods. Vertical dark grey periods show the temperature ramp.

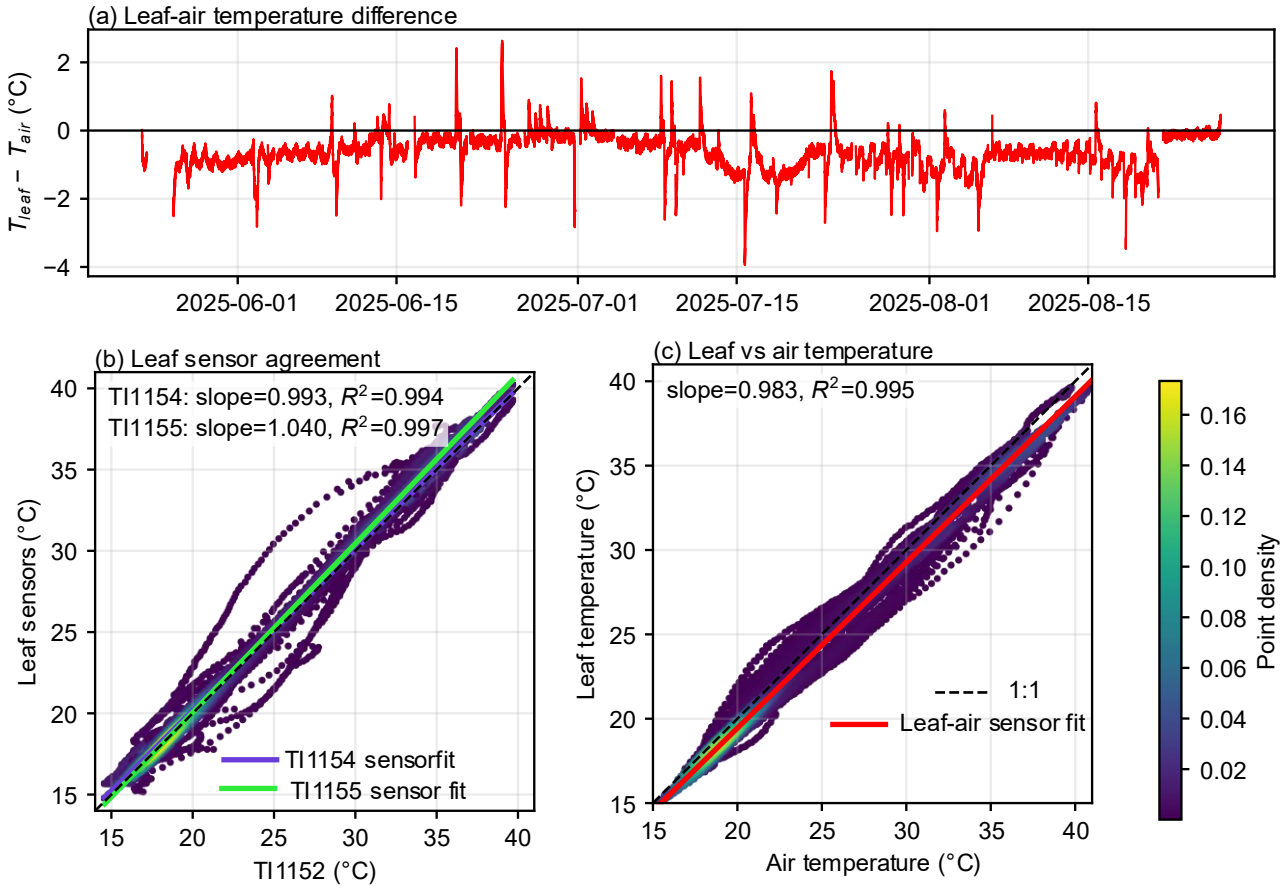


Figure S14 Comparison of leaf and air temperature measurements in the plant chamber. (a) Time series of the leaf–air temperature difference (b) pairwise comparison among leaf temperature sensors (c) relationship between mean leaf and air temperature with regression fit and 1:1 reference line.

Leaf temperature sensors (TI1154 and TI1155) showed a good agreement across the temperature range (15–40 °C), with near 1:1 relationships (R^2 =0.99), and show minimal systematic bias and high measurement consistency among the two sensors. While leaf temperature was strongly correlated with air temperature (R^2 =0.99). Generally, leaf temperature was ~0.5-1.5 °C lower than air temperature during warm periods (>30°C), which could be due to evapotranspiration cooling.

07. Cluster-resolved stress fingerprints

Table S2: Chestnut cluster fingerprint ions and their mean emissions. The ions are the key ions of the UWFCM clusters shown in Fig. 3a, listed by cluster. Emissions are means ± standard deviation over each stress window in nmol m^{-2} s^{-1}; the value in brackets is the fold change compared to the prestress, with ↑ an increase and ↓ a decrease. An ion that is a key ion of more than one cluster appears once per cluster.

m/z	Ion	Cluster	Membership	Share (%)	Prestress	Heat	Heat+O_3
95.04914	$C_6H_7O^+$	Pre-stress (C1)	1.00	71.1	0.095 ± 0.054	0.151 ± 0.054 (~1.8×↑)	0.074 ± 0.026 (~1.2×↓)
107.0855	$C_8H_{11}^+$	Pre-stress (C1)	0.99	2.9	(5.9 ± 5.4) × 10^{-4}	0.0034 ± 0.0013 (~11.2×↑)	0.00219 ± 0.00066 (~8.1×↑)
109.0284	$C_6H_5O_2^+$	Pre-stress (C1)	1.00	12.5	0.035 ± 0.018	0.0090 ± 0.0026 (~3.5×↓)	0.00658 ± 0.00097 (~5.3×↓)
173.0081	$C_6H_5O_6^+$	Pre-stress (C1)	1.00	2.6	0.00113 ± 0.00060	(4.3 ± 1.5) × 10^{-4} (~3.1×↓)	(2.98 ± 0.73) × 10^{-4} (~4.0×↓)

71.08553	$C_5H_{11}^+$	Heat stress (C2)	0.60	12.8	0.036 ± 0.028	0.143 ± 0.071 (~5.8×↑)	0.054 ± 0.021 (~2.1×↑)
85.06479	$C_5H_9O^+$	Heat stress (C2)	0.71	5.2	0.024 ± 0.021	0.065 ± 0.029 (~3.7×↑)	0.027 ± 0.011 (~1.5×↑)
85.10118	$C_6H_{13}^+$	Heat stress (C2)	0.95	2.0	0.0057 ± 0.0050	0.0192 ± 0.0092 (~4.7×↑)	0.0087 ± 0.0032 (~2.1×↑)
99.08044	$C_6H_{11}O^+$	Heat stress (C2)	0.49	3.1	0.020 ± 0.017	0.050 ± 0.021 (~3.3×↑)	0.036 ± 0.013 (~2.3×↑)
101.0597	$C_5H_9O_2^+$	Heat stress (C2)	0.39	3.2	0.035 ± 0.036	0.065 ± 0.024 (~2.5×↑)	0.031 ± 0.010 (~1.1×↑)
105.0699	$C_8H_9^+$	Heat stress (C2)	0.75	2.0	0.0070 ± 0.0064	0.022 ± 0.010 (~4.8×↑)	0.0178 ± 0.0063 (~3.8×↑)
137.1325	$C_{10}H_{17}^+$	Heat stress (C2)	0.56	4.6	0.022 ± 0.012	0.078 ± 0.038 (~3.5×↑)	0.0252 ± 0.0092 (~1.4×↑)
167.0653	Not assigned	Heat stress (C2)	0.77	8.9	0.043 ± 0.051	0.095 ± 0.033 (~4.8×↑)	0.048 ± 0.018 (~2.4×↑)
171.1380	Not assigned	Heat stress (C2)	0.70	1.8	0.0078 ± 0.0068	0.023 ± 0.012 (~4.1×↑)	0.0093 ± 0.0033 (~1.6×↑)
205.1951	$C_{15}H_{25}^+$	Heat stress (C2)	0.93	13.6	0.0016 ± 0.0018	0.0146 ± 0.0057 (~21.9×↑)	0.0103 ± 0.0032 (~16.5×↑)
67.05423	$C_5H_7^+$	Stress factor (C3)	0.76	5.8	0.022 ± 0.014	0.032 ± 0.013 (~1.8×↑)	0.0130 ± 0.0047 (~1.4×↓)
81.03349	$C_5H_5O^+$	Stress factor (C3)	0.68	3.1	0.0145 ± 0.0070	0.0179 ± 0.0072 (~1.4×↑)	0.0068 ± 0.0021 (~2.0×↓)
95.04914	$C_6H_7O^+$	Stress factor (C3)	0.47	12.6	0.095 ± 0.054	0.151 ± 0.054 (~1.8×↑)	0.074 ± 0.026 (~1.2×↓)
111.0441	$C_6H_7O_2^+$	Stress factor (C3)	0.57	1.1	0.043 ± 0.028	0.083 ± 0.027 (~2.3×↑)	0.041 ± 0.014 (~1.1×↑)
117.0182	$C_4H_5O_4^+$	Stress factor (C3)	0.78	0.3	0.00130 ± 0.00061	0.00175 ± 0.00060 (~1.6×↑)	$(9.4 \pm 2.9) \times 10^{-4}$ (~1.3×↓)
119.0855	$C_9H_{11}^+$	Stress factor (C3)	0.94	33.5	0.0062 ± 0.0048	0.0120 ± 0.0050 (~2.8×↑)	0.0053 ± 0.0017 (~1.2×↑)
123.1168	$C_9H_{15}^+$	Stress factor (C3)	0.62	2.5	0.0140 ± 0.0095	0.0149 ± 0.0060 (~1.3×↑)	0.0055 ± 0.0019 (~2.1×↓)
125.1325	$C_9H_{17}^+$	Stress factor (C3)	0.39	0.7	0.0045 ± 0.0033	0.0078 ± 0.0038 (~2.0×↑)	0.00202 ± 0.00078 (~1.8×↓)
135.1168	$C_{10}H_{15}^+$	Stress factor (C3)	0.68	12.5	0.0055 ± 0.0039	0.0077 ± 0.0033 (~1.8×↑)	0.0030 ± 0.0010 (~1.4×↓)
137.0597	$C_8H_9O_2^+$	Stress factor (C3)	0.62	0.8	0.0039 ± 0.0029	0.0055 ± 0.0022 (~1.9×↑)	0.00232 ± 0.00079 (~1.4×↓)
92.06205	Not assigned	Background (C4)	0.70	19.9	0.10 ± 0.10	0.201 ± 0.071 (~3.4×↑)	0.091 ± 0.032 (~1.5×↑)
113.0961	$C_7H_{13}O^+$	Background (C4)	0.56	1.2	0.0065 ± 0.0054	0.0164 ± 0.0072 (~3.3×↑)	0.0065 ± 0.0024 (~1.2×↑)
119.0855	$C_9H_{11}^+$	Background (C4)	0.83	1.4	0.0062 ± 0.0048	0.0120 ± 0.0050 (~2.8×↑)	0.0053 ± 0.0017 (~1.2×↑)
121.0284	$C_7H_5O_2^+$	Background (C4)	0.45	5.4	0.0026 ± 0.0015	0.00240 ± 0.00062 (~1.1×↑)	0.00129 ± 0.00040 (~1.8×↓)
121.0648	$C_8H_9O^+$	Background (C4)	0.86	2.2	0.0090 ± 0.0070	0.0183 ± 0.0081 (~2.9×↑)	0.0081 ± 0.0032 (~1.2×↑)
129.0910	$C_7H_{13}O_2^+$	Background (C4)	0.82	1.4	0.0068 ± 0.0055	0.0124 ± 0.0050 (~2.5×↑)	0.0051 ± 0.0017 (~1.1×↓)
129.1274	$C_8H_{17}O^+$	Background (C4)	0.77	1.6	0.0070 ± 0.0054	0.0149 ± 0.0076 (~2.6×↑)	0.0062 ± 0.0023 (~1.1×↑)
142.0228	Not assigned	Background (C4)	0.76	3.3	$(5.0 \pm 2.4) \times 10^{-4}$	$(6.3 \pm 2.4) \times 10^{-4}$ (~1.4×↑)	$(3.16 \pm 0.92) \times 10^{-4}$ (~1.5×↓)

165.0182	$C_8H_5O_4^+$	Background (C4)	0.83	3.5	$(8.0 \pm 4.1) \times 10^{-4}$	$(5.6 \pm 2.2) \times 10^{-4}$ (~1.3×↓)	$(2.48 \pm 0.57) \times 10^{-4}$ (~3.0×↓)
63.02630	$C_2H_7S^+$	Heat & O3 (C5)	0.96	2.3	0.0028 ± 0.0024	0.0162 ± 0.0054 (~12.0×↑)	0.0092 ± 0.0027 (~7.2×↑)
71.04914	$C_4H_7O^+$	Heat & O3 (C5)	0.97	3.1	0.026 ± 0.027	0.156 ± 0.044 (~15.6×↑)	0.121 ± 0.039 (~12.3×↑)
73.06479	$C_4H_9O^+$	Heat & O3 (C5)	0.32	10.0	0.012 ± 0.012	0.098 ± 0.035 (~22.4×↑)	0.074 ± 0.027 (~18.2×↑)
87.08044	$C_5H_{11}O^+$	Heat & O3 (C5)	0.65	4.6	0.009 ± 0.013	0.046 ± 0.022 (~3.7×↑)	0.0237 ± 0.0095 (~2.1×↑)
101.0597	$C_5H_9O_2^+$	Heat & O3 (C5)	0.47	5.6	0.035 ± 0.036	0.065 ± 0.024 (~2.5×↑)	0.031 ± 0.010 (~1.1×↑)
137.1325	$C_{10}H_{17}^+$	Heat & O3 (C5)	0.99	14.5	0.022 ± 0.012	0.078 ± 0.038 (~3.5×↑)	0.0252 ± 0.0092 (~1.4×↑)
205.1951	$C_{15}H_{25}^+$	Heat & O3 (C5)	0.99	2.1	0.0016 ± 0.0018	0.0146 ± 0.0057 (~21.9×↑)	0.0103 ± 0.0032 (~16.5×↑)
207.1743	$C_{14}H_{23}O^+$	Heat & O3 (C5)	0.96	0.6	$(7.6 \pm 7.6) \times 10^{-4}$	0.0045 ± 0.0023 (~11.2×↑)	0.00247 ± 0.00084 (~6.2×↑)
239.1067	$C_{16}H_{15}O_2^+$	Heat & O3 (C5)	0.99	1.2	0.0014 ± 0.0019	0.0080 ± 0.0034 (~23.5×↑)	0.0041 ± 0.0017 (~11.5×↑)
273.2577	$C_{20}H_{33}^+$	Heat & O3 (C5)	0.96	2.0	$(3.3 \pm 3.8) \times 10^{-4}$	0.00189 ± 0.00088 (~15.0×↑)	$(9.3 \pm 3.1) \times 10^{-4}$ (~6.9×↑)

195

Table S3 Linden cluster fingerprint ions and their mean emissions. The ions are the key ions of the UWFCM clusters shown in Fig. 3a, listed by cluster. Emissions are means ± standard deviation over each stress window in nmol m^{-2} s^{-1}; the value in brackets is the fold change compared to the prestress, with ↑ an increase and ↓ a decrease. An ion that is a key ion of more than one cluster appears once per cluster.

m/z	Ion	Cluster	Membership	Share (%)	Prestress	Heat	Heat+O_3
59.04914	$C_3H_7O^+$	Pre-stress (C1)	0.47	17.3	0.29 ± 0.15	0.188 ± 0.057 (~1.6×↓)	0.124 ± 0.038 (~2.1×↓)
63.02630	$C_2H_7S^+$	Pre-stress (C1)	0.40	1.8	0.025 ± 0.016	0.033 ± 0.011 (~1.8×↑)	0.0102 ± 0.0029 (~1.8×↓)
71.04914	$C_4H_7O^+$	Pre-stress (C1)	0.92	18.1	0.14 ± 0.11	0.047 ± 0.018 (~2.2×↓)	0.031 ± 0.011 (~2.8×↓)
71.08553	$C_5H_{11}^+$	Pre-stress (C1)	0.39	2.4	0.050 ± 0.034	0.036 ± 0.035 (~2.3×↓)	0.0067 ± 0.0043 (~4.6×↓)
75.04406	$C_3H_7O_2^+$	Pre-stress (C1)	0.80	8.0	0.061 ± 0.039	0.071 ± 0.054 (~1.1×↓)	0.028 ± 0.012 (~1.3×↓)
79.05423	$C_6H_7^+$	Pre-stress (C1)	0.39	1.9	0.041 ± 0.015	0.0239 ± 0.0054 (~1.6×↓)	0.0154 ± 0.0023 (~2.3×↓)
85.06479	$C_5H_9O^+$	Pre-stress (C1)	0.71	3.2	0.028 ± 0.022	0.032 ± 0.025 (~1.2×↓)	0.0087 ± 0.0053 (~1.8×↓)
95.04914	$C_6H_7O^+$	Pre-stress (C1)	0.52	7.4	0.121 ± 0.052	0.067 ± 0.031 (~2.3×↓)	0.0418 ± 0.0085 (~2.5×↓)
111.0441	$C_6H_7O_2^+$	Pre-stress (C1)	0.62	6.2	0.072 ± 0.053	0.060 ± 0.031 (~1.1×↓)	0.031 ± 0.010 (~1.3×↓)
115.0754	Not assigned	Pre-stress (C1)	0.59	2.7	0.025 ± 0.017	0.037 ± 0.026 (~1.5×↑)	0.0092 ± 0.0052 (~1.8×↓)
55.01784	$C_3H_3O^+$	Heat stress (C2)	0.56	5.6	0.0104 ± 0.0029	0.027 ± 0.016 (~1.9×↑)	0.0111 ± 0.0025 (~1.3×↑)
99.08044	$C_6H_{11}O^+$	Heat stress (C2)	0.45	2.5	0.022 ± 0.016	0.041 ± 0.028 (~1.9×↑)	0.0101 ± 0.0052 (~1.4×↓)
101.0233	$C_4H_5O_3^+$	Heat stress (C2)	0.87	12.4	0.028 ± 0.011	0.122 ± 0.077 (~3.5×↑)	0.046 ± 0.015 (~2.3×↑)

121.1012	$C_9H_{13}^+$	Heat stress (C2)	0.79	0.8	0.0030 ± 0.0022	0.0086 ± 0.0042 (~3.1×↑)	0.00227 ± 0.00073 (~1.2×↑)
127.0395	$C_6H_7O_3^+$	Heat stress (C2)	0.78	2.2	0.0052 ± 0.0018	0.023 ± 0.014 (~3.3×↑)	0.0133 ± 0.0044 (~3.3×↑)
129.0182	$C_5H_5O_4^+$	Heat stress (C2)	0.92	0.8	0.00188 ± 0.00065	0.0072 ± 0.0043 (~2.9×↑)	0.00315 ± 0.00078 (~2.1×↑)
137.1325	$C_{10}H_{17}^+$	Heat stress (C2)	0.52	30.9	0.036 ± 0.022	0.072 ± 0.037 (~2.0×↑)	0.0289 ± 0.0098 (~1.1×↓)
139.0390	$C_7H_7O_3^+$	Heat stress (C2)	0.75	1.8	0.0071 ± 0.0033	0.018 ± 0.010 (~2.2×↑)	0.0088 ± 0.0022 (~1.8×↑)
149.0233	$C_8H_5O_3^+$	Heat stress (C2)	0.93	1.2	0.0029 ± 0.0011	0.0105 ± 0.0061 (~3.1×↑)	0.0051 ± 0.0016 (~2.4×↑)
71.04914	$C_4H_7O^+$	Stress factor (C3)	0.81	17.7	0.14 ± 0.11	0.047 ± 0.018 (~2.2×↓)	0.031 ± 0.011 (~2.8×↓)
71.08553	$C_5H_{11}^+$	Stress factor (C3)	0.57	5.6	0.050 ± 0.034	0.036 ± 0.035 (~2.3×↓)	0.0067 ± 0.0043 (~4.6×↓)
73.06479	$C_4H_9O^+$	Stress factor (C3)	0.95	8.9	0.071 ± 0.049	0.0128 ± 0.0037 (~4.1×↓)	0.0101 ± 0.0027 (~5.3×↓)
87.08044	$C_5H_{11}O^+$	Stress factor (C3)	0.67	1.3	0.014 ± 0.012	0.0006 ± 0.0032 (~3.9×↓)	−0.00229 ± 0.00072 (~NA)
92.06205	Not assigned	Stress factor (C3)	0.84	15.1	0.16 ± 0.13	0.0088 ± 0.0077 (~11.4×↓)	0.008 ± 0.013 (~20.0×↓)
96.01138	Not assigned	Stress factor (C3)	0.97	1.0	0.0073 ± 0.0050	0.0019 ± 0.0010 (~3.8×↓)	0.00106 ± 0.00031 (~4.7×↓)
107.0491	$C_7H_7O^+$	Stress factor (C3)	0.96	7.6	0.053 ± 0.027	0.017 ± 0.012 (~3.8×↓)	0.0066 ± 0.0027 (~6.0×↓)
115.1117	Not assigned	Stress factor (C3)	0.91	1.0	0.0075 ± 0.0043	0.0025 ± 0.0022 (~4.8×↓)	$(6.2 \pm 4.2) \times 10^{-4}$ (~9.5×↓)
121.0648	$C_8H_9O^+$	Stress factor (C3)	0.42	1.1	0.0146 ± 0.0085	0.0082 ± 0.0066 (~2.0×↓)	0.0024 ± 0.0013 (~4.3×↓)
165.0910	$C_{10}H_{13}O_2^+$	Stress factor (C3)	0.98	1.8	0.0129 ± 0.0086	0.0039 ± 0.0021 (~2.5×↓)	0.00125 ± 0.00067 (~6.3×↓)
55.01784	$C_3H_3O^+$	Background (C4)	0.46	2.8	0.0104 ± 0.0029	0.027 ± 0.016 (~1.9×↑)	0.0111 ± 0.0025 (~1.3×↑)
65.03858	$C_5H_5^+$	Background (C4)	0.64	1.0	0.00242 ± 0.00042	0.0070 ± 0.0040 (~1.9×↑)	0.00293 ± 0.00077 (~1.3×↑)
81.03349	$C_5H_5O^+$	Background (C4)	0.95	8.2	0.0158 ± 0.0031	0.035 ± 0.017 (~1.9×↑)	0.0231 ± 0.0054 (~1.7×↑)
109.0284	$C_6H_5O_2^+$	Background (C4)	0.89	23.6	0.0410 ± 0.0053	0.110 ± 0.047 (~1.7×↑)	0.0736 ± 0.0089 (~1.7×↑)
110.0329	Not assigned	Background (C4)	0.91	8.9	0.0177 ± 0.0026	0.040 ± 0.016 (~1.5×↑)	0.0237 ± 0.0036 (~1.3×↑)
121.0284	$C_7H_5O_2^+$	Background (C4)	0.31	0.5	0.0026 ± 0.0012	0.0072 ± 0.0036 (~3.6×↑)	0.00393 ± 0.00056 (~2.0×↑)
125.0233	$C_6H_5O_3^+$	Background (C4)	0.94	8.8	0.0151 ± 0.0012	0.039 ± 0.018 (~1.7×↑)	0.0256 ± 0.0034 (~1.7×↑)
126.0275	Not assigned	Background (C4)	0.97	1.0	0.00156 ± 0.00019	0.0042 ± 0.0020 (~1.9×↑)	0.00264 ± 0.00042 (~1.8×↑)
141.0182	$C_6H_5O_4^+$	Background (C4)	0.98	2.8	0.00462 ± 0.00026	0.0121 ± 0.0061 (~1.7×↑)	0.0076 ± 0.0012 (~1.7×↑)
81.06988	$C_6H_9^+$	Extreme heat (C5)	0.97	5.0	0.037 ± 0.031	0.27 ± 0.21 (~5.0×↑)	0.043 ± 0.022 (~1.8×↑)
83.08553	$C_6H_{11}^+$	Extreme heat (C5)	0.88	11.8	0.061 ± 0.037	0.24 ± 0.20 (~2.5×↑)	0.051 ± 0.024 (~1.1×↑)
99.04406	$C_5H_7O_2^+$	Extreme heat (C5)	0.97	3.5	0.011 ± 0.011	0.067 ± 0.047 (~7.6×↑)	0.018 ± 0.011 (~3.3×↑)

101.0597	$C_5H_9O_2^+$	Extreme heat (C5)	0.50	2.7	0.047 ± 0.038	0.078 ± 0.066 (~1.3×↑)	0.0084 ± 0.0089 (~2.3×↓)
105.0699	$C_8H_9^+$	Extreme heat (C5)	0.86	3.5	0.0098 ± 0.0073	0.083 ± 0.090 (~8.0×↑)	0.0120 ± 0.0079 (~1.9×↑)
123.1168	$C_9H_{15}^+$	Extreme heat (C5)	0.99	4.5	0.0080 ± 0.0052	0.093 ± 0.075 (~9.1×↑)	0.0141 ± 0.0062 (~2.9×↑)
143.1430	$C_9H_{19}O^+$	Extreme heat (C5)	1.00	3.2	0.0089 ± 0.0054	0.061 ± 0.051 (~4.7×↑)	0.0147 ± 0.0074 (~2.1×↑)
203.1794	$C_{15}H_{23}^+$	Extreme heat (C5)	0.97	3.0	0.0024 ± 0.0017	0.067 ± 0.060 (~22.2×↑)	0.0070 ± 0.0026 (~5.3×↑)
205.1951	$C_{15}H_{25}^+$	Extreme heat (C5)	0.99	13.4	0.015 ± 0.011	0.093 ± 0.055 (~8.2×↑)	0.031 ± 0.010 (~2.9×↑)
273.2577	$C_{20}H_{33}^+$	Extreme heat (C5)	0.97	22.4	0.0032 ± 0.0047	0.52 ± 0.56 (~170.6×↑)	0.051 ± 0.028 (~38.6×↑)

200

08. Detection limit of the FUSION PTR-TOF-MS compounds

Table S4. Limits of detection (LOD) of the ions of chestnut and linden emissions. Values are the median ± standard deviation (ppbv) of all 1-min LOD values during the measurement period of linden and chestnut.

m/z	Ion	Chestnut LOD median ± SD (ppbv)	Linden LOD median ± SD (ppbv)	m/z	Ion	Chestnut LOD median ± SD (ppbv)	Linden LOD median ± SD (ppbv)
33.03349	CH_5O^+	0.03 ± 0.14	0.034 ± 0.049	145.1223	$C_8H_{17}O_2^+$	0.0003 ± 0.0014	$(1.2 \pm 1.2) \times 10^{-4}$
39.02293	$C_3H_3^+$	—	0.0027 ± 0.0037	146.0154	Not assigned	$(1.3 \pm 2.8) \times 10^{-4}$	$(5.2 \pm 4.8) \times 10^{-5}$
41.03858	$C_3H_5^+$	0.009 ± 0.021	$(4.0 \pm 9.7) \times 10^{-4}$	146.0532	Not assigned	$(1.8 \pm 7.0) \times 10^{-4}$	$(8.0 \pm 6.6) \times 10^{-5}$
42.01002	$C_2H_2O^+$	$(9.0 \pm 8.2) \times 10^{-4}$	$(5.7 \pm 5.9) \times 10^{-4}$	146.9763	Not assigned	—	$(6.4 \pm 5.5) \times 10^{-5}$
43.01784	$C_2H_3O^+$	—	0.0053 ± 0.0084	147.0297	$C_6H_{11}S_2^+$	—	$(8.9 \pm 4.6) \times 10^{-5}$
43.05423	$C_3H_7^+$	—	0.0068 ± 0.0060	148.0435	Not assigned	$(2.4 \pm 4.9) \times 10^{-4}$	—
44.97918	Not assigned	—	0.0010 ± 0.0067	149.0233	$C_8H_5O_3^+$	—	$(3.0 \pm 2.8) \times 10^{-4}$
45.03349	$C_2H_5O^+$	0.003 ± 0.011	0.0004 ± 0.0022	149.0961	Not assigned	—	$(1.4 \pm 1.7) \times 10^{-4}$
46.02874	CH_4NO^+	0.004 ± 0.022	0.0038 ± 0.0052	149.1325	$C_{11}H_{17}^+$	—	$(2.0 \pm 3.6) \times 10^{-4}$
47.01276	$CH_3O_2^+$	0.0019 ± 0.0030	$(7.5 \pm 8.6) \times 10^{-4}$	150.0913	Not assigned	—	$(8.0 \pm 6.0) \times 10^{-5}$
47.99735	Not assigned	—	$(2.4 \pm 2.2) \times 10^{-4}$	151.0754	Not assigned	0.0005 ± 0.0016	$(2.4 \pm 1.8) \times 10^{-4}$
49.01065	CH_5S^+	—	$(7.5 \pm 8.4) \times 10^{-5}$	151.1117	Not assigned	0.0003 ± 0.0015	—
49.02841	$CH_5O_2^+$	—	$(1.52 \pm 0.78) \times 10^{-4}$	152.0706	$C_8H_{10}NO_2^+$	0.0003 ± 0.0012	$(9.3 \pm 6.5) \times 10^{-5}$
51.02293	$C_4H_3^+$	—	$(1.5 \pm 5.3) \times 10^{-4}$	153.0546	$C_8H_9O_3^+$	0.0002 ± 0.0012	$(2.2 \pm 1.8) \times 10^{-4}$
52.03075	$C_4H_4^+$	$(2.5 \pm 6.1) \times 10^{-4}$	—	154.0499	$C_7H_8NO_3^+$	—	$(1.6 \pm 1.2) \times 10^{-4}$
53.00219	C_3HO^+	—	$(2.8 \pm 2.5) \times 10^{-4}$	155.0339	$C_7H_7O_4^+$	—	$(2.6 \pm 2.1) \times 10^{-4}$
53.03858	$C_4H_5^+$	—	$(4.1 \pm 6.5) \times 10^{-4}$	155.1067	$C_9H_{15}O_2^+$	0.0007 ± 0.0029	—
54.00561	Not assigned	—	$(7.2 \pm 6.1) \times 10^{-5}$	155.1430	$C_{10}H_{19}O^+$	0.0004 ± 0.0018	—
54.03383	$C_3H_4N^+$	—	$(2.0 \pm 1.4) \times 10^{-4}$	157.0495	$C_7H_9O_4^+$	0.0008 ± 0.0023	$(3.6 \pm 3.1) \times 10^{-4}$
55.01784	$C_3H_3O^+$	—	$(2.8 \pm 2.7) \times 10^{-4}$	157.0859	$C_8H_{13}O_3^+$	—	$(2.1 \pm 1.8) \times 10^{-4}$
55.05423	$C_4H_7^+$	0.006 ± 0.019	0.0011 ± 0.0017	157.1587	Not assigned	—	$(1.8 \pm 1.5) \times 10^{-4}$
56.05758	$^{13}CC_3H_7^+$	0.0012 ± 0.0015	—	158.0448	$C_6H_8NO_4^+$	0.0004 ± 0.0013	—
57.06988	$C_4H_9^+$	0.0014 ± 0.0018	$(1.8 \pm 6.1) \times 10^{-4}$	159.0288	$C_6H_7O_5^+$	—	$(1.8 \pm 1.5) \times 10^{-4}$
58.02874	$C_2H_4NO^+$	—	$(1.3 \pm 1.3) \times 10^{-4}$	159.1016	Not assigned	0.0003 ± 0.0011	$(1.07 \pm 0.83) \times 10^{-4}$
58.04132	$C_3H_6O^+$	—	$(2.3 \pm 2.8) \times 10^{-4}$	161.0445	$C_6H_9O_5^+$	—	$(1.5 \pm 1.1) \times 10^{-4}$
59.04914	$C_3H_7O^+$	—	$(6.6 \pm 5.4) \times 10^{-4}$	161.1073	$C_{10}H_{13}N_2^+$	0.0003 ± 0.0012	—
61.02841	$C_2H_5O_2^+$	—	0.0012 ± 0.0022	161.1325	$C_{12}H_{17}^+$	$(3.1 \pm 5.9) \times 10^{-4}$	—
63.02630	$C_2H_7S^+$	0.0010 ± 0.0018	$(5.2 \pm 4.5) \times 10^{-4}$	163.1481	$C_{12}H_{19}^+$	0.0003 ± 0.0010	—
65.03858	$C_5H_5^+$	—	$(2.7 \pm 1.4) \times 10^{-4}$	165.0182	$C_8H_5O_4^+$	—	$(2.2 \pm 1.5) \times 10^{-4}$
67.05423	$C_5H_7^+$	0.0005 ± 0.0014	—	165.0910	$C_{10}H_{13}O_2^+$	0.0004 ± 0.0013	$(1.7 \pm 1.3) \times 10^{-4}$
68.04948	$C_4H_6N^+$	$(6.7 \pm 9.3) \times 10^{-4}$	$(2.8 \pm 2.0) \times 10^{-4}$	165.1274	$C_{11}H_{17}O^+$	0.0003 ± 0.0011	—
69.06988	$C_5H_9^+$	0.0052 ± 0.0067	0.0023 ± 0.0022	165.1638	$C_{12}H_{21}^+$	$(3.2 \pm 9.6) \times 10^{-4}$	—
71.04914	$C_4H_7O^+$	0.0036 ± 0.0050	0.0018 ± 0.0019	166.0863	$C_9H_{12}NO_2^+$	$(1.9 \pm 6.6) \times 10^{-4}$	$(7.8 \pm 5.7) \times 10^{-5}$
71.08553	$C_5H_{11}^+$	0.0099 ± 0.0097	0.0014 ± 0.0013	167.0653	Not assigned	0.0008 ± 0.0027	—
73.06479	$C_4H_9O^+$	0.0025 ± 0.0033	0.0009 ± 0.0012	169.1223	$C_{10}H_{17}O_2^+$	0.0004 ± 0.0011	—

74.06004	$C_3H_8NO^+$	0.0031 ± 0.0058	—	169.1587	$C_{11}H_{21}O^+$	$(3.1 \pm 8.2) \times 10^{-4}$	—
75.04406	$C_3H_7O_2^+$	0.0013 ± 0.0034	$(4.7 \pm 4.0) \times 10^{-4}$	171.1380	Not assigned	0.0005 ± 0.0013	$(1.9 \pm 1.9) \times 10^{-4}$
78.04640	Not assigned	0.001 ± 0.025	—	171.1743	Not assigned	0.0004 ± 0.0011	$(1.6 \pm 1.3) \times 10^{-4}$
79.05423	$C_6H_7^+$	0.001 ± 0.012	$(9.6 \pm 7.1) \times 10^{-4}$	173.0081	$C_6H_5O_6^+$	0.0004 ± 0.0016	—
80.02075	Not assigned	$(2.6 \pm 7.6) \times 10^{-4}$	$(0.9 \pm 1.1) \times 10^{-4}$	173.0445	$C_7H_9O_5^+$	0.0004 ± 0.0013	—
81.03349	$C_5H_5O^+$	0.003 ± 0.014	0.0015 ± 0.0012	173.0808	$C_8H_{13}O_4^+$	$(3.0 \pm 9.3) \times 10^{-4}$	—
81.06988	$C_6H_9^+$	—	0.0025 ± 0.0022	173.1172	$C_9H_{17}O_3^+$	$(2.6 \pm 6.7) \times 10^{-4}$	$(1.13 \pm 0.84) \times 10^{-4}$
82.00644	Not assigned	—	$(3.0 \pm 2.6) \times 10^{-4}$	173.1536	$C_{10}H_{21}O_2^+$	0.0004 ± 0.0013	—
83.08553	$C_6H_{11}^+$	0.0023 ± 0.0065	$(9.0 \pm 9.1) \times 10^{-4}$	175.1481	Not assigned	$(2.0 \pm 7.5) \times 10^{-4}$	—
85.06479	$C_5H_9O^+$	0.0062 ± 0.0086	0.0015 ± 0.0016	177.1638	$C_{13}H_{21}^+$	0.0003 ± 0.0011	—
85.10118	$C_6H_{13}^+$	0.0017 ± 0.0054	$(7.6 \pm 6.4) \times 10^{-4}$	178.9892	Not assigned	—	$(1.01 \pm 0.90) \times 10^{-4}$
86.06004	$C_4H_8NO^+$	0.0014 ± 0.0051	—	179.0339	$C_9H_7O_4^+$	$(2.4 \pm 7.9) \times 10^{-4}$	$(1.40 \pm 0.92) \times 10^{-4}$
87.00767	$C_3H_3O_3^+$	—	$(6.2 \pm 5.6) \times 10^{-4}$	179.0703	$C_{10}H_{11}O_3^+$	$(2.5 \pm 9.5) \times 10^{-4}$	—
87.04406	$C_4H_7O_2^+$	0.0064 ± 0.0081	0.0011 ± 0.0012	179.1067	$C_{11}H_{15}O_2^+$	$(2.6 \pm 7.0) \times 10^{-4}$	$(9.0 \pm 8.2) \times 10^{-5}$
87.08044	$C_5H_{11}O^+$	0.0106 ± 0.0095	0.0014 ± 0.0016	179.1430	$C_{12}H_{19}O^+$	$(2.4 \pm 5.7) \times 10^{-4}$	—
88.04021	Not assigned	0.0017 ± 0.0029	—	179.1794	$C_{13}H_{23}^+$	$(2.7 \pm 9.1) \times 10^{-4}$	—
90.01857	$C_2H_4NO_3^+$	—	$(2.1 \pm 1.8) \times 10^{-4}$	181.0026	$C_7H_5ClF_3^+$	—	$(1.6 \pm 1.3) \times 10^{-4}$
92.06205	Not assigned	0.0016 ± 0.0064	$(7.5 \pm 6.0) \times 10^{-4}$	181.0859	$C_{10}H_{13}O_3^+$	$(3.8 \pm 8.8) \times 10^{-4}$	$(1.4 \pm 1.1) \times 10^{-4}$
94.04132	$C_6H_6O^+$	—	$(7.0 \pm 7.0) \times 10^{-4}$	181.1223	$C_{11}H_{17}O_2^+$	0.0005 ± 0.0011	$(1.24 \pm 0.73) \times 10^{-4}$
95.01276	$C_5H_3O_2^+$	—	0.0006 ± 0.0011	181.1587	$C_{12}H_{21}O^+$	$(2.8 \pm 7.9) \times 10^{-4}$	$(9.9 \pm 8.5) \times 10^{-5}$
95.04914	$C_6H_7O^+$	0.004 ± 0.026	0.0015 ± 0.0013	183.0347	$CH_{11}O_{10}^+$	—	$(1.5 \pm 1.3) \times 10^{-4}$
96.01138	Not assigned	—	$(1.5 \pm 3.2) \times 10^{-4}$	183.0804	$C_{13}H_{11}O^+$	0.0004 ± 0.0013	—
96.05243	Not assigned	—	$(5.2 \pm 3.7) \times 10^{-4}$	183.1016	$C_{10}H_{15}O_3^+$	0.0006 ± 0.0018	—
97.06479	$C_6H_9O^+$	0.003 ± 0.011	—	183.1380	$C_{11}H_{19}O_2^+$	$(3.2 \pm 7.9) \times 10^{-4}$	—
99.04406	$C_5H_7O_2^+$	0.005 ± 0.012	0.0020 ± 0.0019	183.1743	$C_{12}H_{23}O^+$	$(2.9 \pm 6.4) \times 10^{-4}$	—
99.08044	$C_6H_{11}O^+$	0.0033 ± 0.0085	0.00114 ± 0.00095	185.0043	Not assigned	—	$(1.01 \pm 0.85) \times 10^{-4}$
100.0458	Not assigned	—	$(5.4 \pm 5.0) \times 10^{-4}$	185.0445	$C_8H_9O_5^+$	—	$(1.4 \pm 2.1) \times 10^{-4}$
101.0233	$C_4H_5O_3^+$	—	$(7.4 \pm 6.2) \times 10^{-4}$	185.0808	$C_9H_{13}O_4^+$	0.0004 ± 0.0011	—
101.0597	$C_5H_9O_2^+$	0.013 ± 0.013	0.0026 ± 0.0030	185.1172	$C_{10}H_{17}O_3^+$	$(3.0 \pm 7.0) \times 10^{-4}$	—
101.0961	$C_6H_{13}O^+$	0.0020 ± 0.0063	$(7.6 \pm 7.5) \times 10^{-4}$	185.1536	Not assigned	$(3.2 \pm 8.4) \times 10^{-4}$	$(9.9 \pm 8.7) \times 10^{-5}$
103.0754	$C_5H_{11}O_2^+$	0.0024 ± 0.0038	$(5.6 \pm 4.9) \times 10^{-4}$	185.1900	Not assigned	$(4.0 \pm 9.5) \times 10^{-4}$	$(1.4 \pm 1.1) \times 10^{-4}$
105.0699	$C_8H_9^+$	0.0017 ± 0.0042	$(6.3 \pm 4.8) \times 10^{-4}$	187.0754	$C_{12}H_{11}O_2^+$	—	$(3.0 \pm 2.4) \times 10^{-4}$
107.0491	$C_7H_7O^+$	0.0008 ± 0.0022	$(3.2 \pm 3.7) \times 10^{-4}$	187.1329	$C_{10}H_{19}O_3^+$	$(2.4 \pm 5.7) \times 10^{-4}$	—
107.0855	$C_8H_{11}^+$	0.0005 ± 0.0013	$(3.7 \pm 2.2) \times 10^{-4}$	189.1638	$C_{14}H_{21}^+$	$(2.8 \pm 7.6) \times 10^{-4}$	—
108.0813	$C_7H_{10}N^+$	0.0006 ± 0.0016	—	191.0275	Not assigned	—	$(1.6 \pm 1.4) \times 10^{-4}$
109.0284	$C_6H_5O_2^+$	0.004 ± 0.026	0.0018 ± 0.0014	191.1794	Not assigned	0.0004 ± 0.0012	—
110.0329	Not assigned	0.002 ± 0.013	0.0008 ± 0.0010	193.1223	$C_{12}H_{17}O_2^+$	$(2.3 \pm 5.5) \times 10^{-4}$	$(6.3 \pm 6.2) \times 10^{-5}$
111.0441	$C_6H_7O_2^+$	0.003 ± 0.014	0.00103 ± 0.00086	193.1587	$C_{13}H_{21}O^+$	$(2.5 \pm 5.4) \times 10^{-4}$	—
112.0492	Not assigned	0.0009 ± 0.0025	—	193.1951	$C_{14}H_{25}^+$	$(3.2 \pm 6.3) \times 10^{-4}$	—
113.0961	$C_7H_{13}O^+$	0.0012 ± 0.0029	$(4.9 \pm 3.5) \times 10^{-4}$	195.0171	Not assigned	$(1.9 \pm 3.3) \times 10^{-4}$	$(9.8 \pm 9.7) \times 10^{-5}$
115.0754	Not assigned	0.0023 ± 0.0040	$(7.4 \pm 7.0) \times 10^{-4}$	195.0652	$C_{10}H_{11}O_4^+$	$(2.4 \pm 5.4) \times 10^{-4}$	—
115.1117	Not assigned	0.0010 ± 0.0022	$(3.8 \pm 3.1) \times 10^{-4}$	195.1016	$C_{11}H_{15}O_3^+$	$(2.5 \pm 5.4) \times 10^{-4}$	—
116.0371	Not assigned	0.0007 ± 0.0013	$(2.0 \pm 1.9) \times 10^{-4}$	195.1380	$C_{12}H_{19}O_2^+$	$(2.7 \pm 5.4) \times 10^{-4}$	—
117.0182	$C_4H_5O_4^+$	0.0005 ± 0.0014	—	199.0390	$C_{12}H_7O_3^+$	$(2.9 \pm 8.0) \times 10^{-4}$	$(1.2 \pm 1.3) \times 10^{-4}$
117.0546	$C_5H_9O_3^+$	0.0013 ± 0.0026	—	199.0754	$C_{13}H_{11}O_2^+$	—	$(1.4 \pm 1.5) \times 10^{-4}$
117.0910	$C_6H_{13}O_2^+$	0.0006 ± 0.0011	$(2.4 \pm 1.5) \times 10^{-4}$	199.1329	$C_{11}H_{19}O_3^+$	$(2.3 \pm 6.6) \times 10^{-4}$	—
119.0339	$C_4H_7O_4^+$	—	$(1.8 \pm 1.0) \times 10^{-4}$	199.1693	$C_{12}H_{23}O_2^+$	$(3.1 \pm 4.9) \times 10^{-4}$	—
119.0855	$C_9H_{11}^+$	0.0006 ± 0.0014	$(1.8 \pm 2.1) \times 10^{-4}$	199.2056	$C_{13}H_{27}O^+$	$(3.7 \pm 7.4) \times 10^{-4}$	—
120.0351	Not assigned	$(2.1 \pm 3.7) \times 10^{-4}$	$(7.1 \pm 6.6) \times 10^{-5}$	201.0313	Not assigned	$(2.8 \pm 5.1) \times 10^{-4}$	$(9.4 \pm 9.7) \times 10^{-5}$
121.0284	$C_7H_5O_2^+$	—	$(2.0 \pm 1.3) \times 10^{-4}$	201.1121	$C_{10}H_{17}O_4^+$	$(2.3 \pm 6.1) \times 10^{-4}$	—
121.0648	$C_8H_9O^+$	0.0007 ± 0.0025	$(3.9 \pm 2.9) \times 10^{-4}$	201.1638	$C_{15}H_{21}^+$	$(2.4 \pm 8.7) \times 10^{-4}$	$(1.1 \pm 1.1) \times 10^{-4}$
121.1012	$C_9H_{13}^+$	0.0003 ± 0.0012	$(2.6 \pm 2.3) \times 10^{-4}$	203.1794	$C_{15}H_{23}^+$	0.0005 ± 0.0011	$(2.3 \pm 4.4) \times 10^{-4}$
122.0362	Not assigned	—	$(9.6 \pm 7.9) \times 10^{-5}$	205.1951	$C_{15}H_{25}^+$	$(3.8 \pm 8.4) \times 10^{-4}$	$(3.3 \pm 6.6) \times 10^{-4}$
122.0600	Not assigned	0.0004 ± 0.0014	$(2.0 \pm 1.6) \times 10^{-4}$	207.1016	$C_{12}H_{15}O_3^+$	$(2.3 \pm 6.0) \times 10^{-4}$	—
123.1168	$C_9H_{15}^+$	0.0006 ± 0.0015	$(2.3 \pm 1.9) \times 10^{-4}$	207.1380	$C_{13}H_{19}O_2^+$	$(2.5 \pm 6.8) \times 10^{-4}$	—
125.0233	$C_6H_5O_3^+$	0.0009 ± 0.0088	$(7.9 \pm 5.9) \times 10^{-4}$	207.1743	$C_{14}H_{23}O^+$	$(3.0 \pm 7.0) \times 10^{-4}$	—

125.0961	$C_8H_{13}O^+$	$(0.0 \pm 3.0) \times 10^{-4}$	—	207.2107	$C_{15}H_{27}^+$	$(2.9 \pm 5.5) \times 10^{-4}$	$(1.2 \pm 1.2) \times 10^{-4}$
125.1325	$C_9H_{17}^+$	0.0005 ± 0.0012	$(2.3 \pm 1.8) \times 10^{-4}$	211.0303	Not assigned	$(2 \pm 10) \times 10^{-4}$	—
126.0275	Not assigned	—	$(2.1 \pm 1.6) \times 10^{-4}$	211.1693	$C_{13}H_{23}O_2^+$	$(2.8 \pm 6.0) \times 10^{-4}$	—
127.0395	$C_6H_7O_3^+$	0.0010 ± 0.0026	$(3.9 \pm 2.9) \times 10^{-4}$	211.2056	$C_{14}H_{27}O^+$	$(3.0 \pm 7.7) \times 10^{-4}$	$(1.0 \pm 1.1) \times 10^{-4}$
129.0182	$C_5H_5O_4^+$	—	$(2.4 \pm 2.7) \times 10^{-4}$	212.9919	Not assigned	—	$(9.0 \pm 8.8) \times 10^{-5}$
129.0546	$C_6H_9O_3^+$	0.0012 ± 0.0031	$(4.8 \pm 3.4) \times 10^{-4}$	213.0436	Not assigned	$(2.4 \pm 7.1) \times 10^{-4}$	$(1.0 \pm 1.0) \times 10^{-4}$
129.0910	$C_7H_{13}O_2^+$	0.0008 ± 0.0022	—	213.2213	$C_{14}H_{29}O^+$	$(3.3 \pm 6.7) \times 10^{-4}$	—
129.1274	$C_8H_{17}O^+$	0.0005 ± 0.0020	$(2.3 \pm 2.3) \times 10^{-4}$	217.1951	$C_{16}H_{25}^+$	$(2.7 \pm 5.2) \times 10^{-4}$	—
130.0250	Not assigned	$(3.0 \pm 6.0) \times 10^{-4}$	—	227.1642	$C_{13}H_{23}O_3^+$	$(2.4 \pm 7.4) \times 10^{-4}$	—
130.0932	Not assigned	$(3.1 \pm 8.7) \times 10^{-4}$	—	231.1591	$C_{12}H_{23}O_4^+$	$(1.6 \pm 3.7) \times 10^{-4}$	—
131.0339	$C_5H_7O_4^+$	—	$(2.4 \pm 1.8) \times 10^{-4}$	231.2107	$C_{17}H_{27}^+$	$(2.1 \pm 5.3) \times 10^{-4}$	—
131.1067	Not assigned	0.0004 ± 0.0010	$(1.6 \pm 1.6) \times 10^{-4}$	233.2111	$C_{13}H_{29}O_3^+$	$(2.4 \pm 5.4) \times 10^{-4}$	$(9.4 \pm 7.5) \times 10^{-5}$
132.0808	Not assigned	$(1.7 \pm 9.1) \times 10^{-4}$	—	237.1485	$C_{14}H_{21}O_3^+$	$(2.6 \pm 6.5) \times 10^{-4}$	—
135.0804	Not assigned	—	$(2.4 \pm 2.3) \times 10^{-4}$	239.1067	$C_{16}H_{15}O_2^+$	$(4.8 \pm 9.1) \times 10^{-4}$	—
135.1168	$C_{10}H_{15}^+$	0.0004 ± 0.0024	$(2.0 \pm 2.1) \times 10^{-4}$	239.1528	Not assigned	$(2.4 \pm 4.3) \times 10^{-4}$	—
136.0757	Not assigned	$(2.8 \pm 8.2) \times 10^{-4}$	$(1.20 \pm 0.99) \times 10^{-4}$	239.2006	$C_{15}H_{27}O_2^+$	$(2.1 \pm 3.6) \times 10^{-4}$	—
137.0597	$C_8H_9O_2^+$	0.0006 ± 0.0024	$(3.3 \pm 2.7) \times 10^{-4}$	239.2369	$C_{16}H_{31}O^+$	—	$(1.8 \pm 1.6) \times 10^{-4}$
137.0961	$C_9H_{13}O^+$	0.0006 ± 0.0026	$(2.9 \pm 2.3) \times 10^{-4}$	241.2162	$C_{15}H_{29}O_2^+$	$(2.3 \pm 4.0) \times 10^{-4}$	—
137.1325	$C_{10}H_{17}^+$	0.0004 ± 0.0016	$(3.6 \pm 3.0) \times 10^{-4}$	243.2107	$C_{18}H_{27}^+$	$(2.0 \pm 4.6) \times 10^{-4}$	—
139.0390	$C_7H_7O_3^+$	—	$(4.8 \pm 3.3) \times 10^{-4}$	245.2264	$C_{18}H_{29}^+$	$(2.2 \pm 4.4) \times 10^{-4}$	—
139.1117	$C_9H_{15}O^+$	0.0003 ± 0.0011	—	247.2268	$C_{14}H_{31}O_3^+$	$(2.4 \pm 4.5) \times 10^{-4}$	—
140.0342	$C_6H_6NO_3^+$	—	$(1.8 \pm 1.2) \times 10^{-4}$	249.1849	$C_{16}H_{25}O_2^+$	$(2.3 \pm 4.0) \times 10^{-4}$	$(5.5 \pm 4.2) \times 10^{-5}$
141.0182	$C_6H_5O_4^+$	0.0008 ± 0.0036	$(4.2 \pm 2.8) \times 10^{-4}$	253.1798	$C_{15}H_{25}O_3^+$	—	$(5.2 \pm 5.3) \times 10^{-5}$
141.1274	Not assigned	—	$(2.3 \pm 1.8) \times 10^{-4}$	255.2319	$C_{16}H_{31}O_2^+$	—	$(1.1 \pm 1.4) \times 10^{-4}$
142.0228	Not assigned	—	$(1.4 \pm 1.8) \times 10^{-4}$	257.2264	$C_{19}H_{29}^+$	$(3.4 \pm 4.1) \times 10^{-4}$	—
142.0930	Not assigned	—	$(1.24 \pm 0.89) \times 10^{-4}$	259.2056	$C_{18}H_{27}O^+$	$(2.5 \pm 3.4) \times 10^{-4}$	—
143.0339	$C_6H_7O_4^+$	—	$(3.5 \pm 2.8) \times 10^{-4}$	259.2420	$C_{19}H_{31}^+$	$(2.9 \pm 5.6) \times 10^{-4}$	—
143.1430	$C_9H_{19}O^+$	—	$(2.1 \pm 1.6) \times 10^{-4}$	271.2420	$C_{20}H_{31}^+$	$(2.1 \pm 4.7) \times 10^{-4}$	—
145.0495	$C_6H_9O_4^+$	0.0005 ± 0.0010	$(2.3 \pm 1.8) \times 10^{-4}$	273.2577	$C_{20}H_{33}^+$	$(2.9 \pm 3.2) \times 10^{-4}$	0.0008 ± 0.0027
145.0859	Not assigned	0.0004 ± 0.0017	—				

09. References

(1) Kim, D.-W.; Lee, K. H. A New Validity Measure for Fuzzy C-Means Clustering. **2024**, 1–6. https://doi.org/10.48550/arXiv.2407.06774.

(2) Tsekouras, G. E.; Sarimveis, H. A New Approach for Measuring the Validity of the Fuzzy C-Means Algorithm. *Advances in Engineering Software* **2004**, *35* (8–9), 567–575. https://doi.org/10.1016/j.advengsoft.2004.05.001.

(3) Chen, G.; Wang, X.; Sun, Q.; Tang, Z. Z. Multidimensional Scaling Improves Distance-Based Clustering for Microbiome Data. *Bioinformatics* **2025**, *41* (2). https://doi.org/10.1093/bioinformatics/btaf042.

(4) Wongoutong, C. The Impact of Neglecting Feature Scaling in K-Means Clustering. *PLoS ONE* **2024**, *19* (12), 1–19. https://doi.org/10.1371/journal.pone.0310839.

(5) Wu, R.; Zorn, S. R.; Kang, S.; Kiendler-Scharr, A.; Wahner, A.; Mentel, T. F. Application of Fuzzy C-Means Clustering for Analysis of Chemical Ionization Mass Spectra: Insights into the Gas Phase Chemistry of NO3-Initiated Oxidation of Isoprene. *Atmospheric Measurement Techniques* **2024**, *17* (6), 1811–1835. https://doi.org/10.5194/amt-17-1811-2024.